FACTORS OF SAFETY FOR RICHARDSON EXTRAPOLATION

by

Tao Xing[1] and Fred Stern

IIHR Technical Report No. 469

IIHR—Hydroscience & Engineering
College of Engineering
The University of Iowa
Iowa City, Iowa 52242-1585 USA

March 2009

[1] Current affiliation: Department of Mechanical Engineering, Tuskegee University, Tuskegee, AL 36088

Report Documentation Page		Form Approved OMB No. 0704-0188

Public reporting burden for the collection of information is estimated to average 1 hour per response, including the time for reviewing instructions, searching existing data sources, gathering and maintaining the data needed, and completing and reviewing the collection of information. Send comments regarding this burden estimate or any other aspect of this collection of information, including suggestions for reducing this burden, to Washington Headquarters Services, Directorate for Information Operations and Reports, 1215 Jefferson Davis Highway, Suite 1204, Arlington VA 22202-4302. Respondents should be aware that notwithstanding any other provision of law, no person shall be subject to a penalty for failing to comply with a collection of information if it does not display a currently valid OMB control number.

1. REPORT DATE **MAR 2009**	2. REPORT TYPE	3. DATES COVERED **00-00-2009 to 00-00-2009**
4. TITLE AND SUBTITLE **Factors of Safety for Richardson Extrapolation**		5a. CONTRACT NUMBER
		5b. GRANT NUMBER
		5c. PROGRAM ELEMENT NUMBER
6. AUTHOR(S)		5d. PROJECT NUMBER
		5e. TASK NUMBER
		5f. WORK UNIT NUMBER
7. PERFORMING ORGANIZATION NAME(S) AND ADDRESS(ES) **IIHR?Hydroscience & Engineering,College of Engineering,The University of Iowa,Iowa City,IA,52242-1585**		8. PERFORMING ORGANIZATION REPORT NUMBER
9. SPONSORING/MONITORING AGENCY NAME(S) AND ADDRESS(ES)		10. SPONSOR/MONITOR'S ACRONYM(S)
		11. SPONSOR/MONITOR'S REPORT NUMBER(S)

12. DISTRIBUTION/AVAILABILITY STATEMENT
Approved for public release; distribution unlimited

13. SUPPLEMENTARY NOTES

14. ABSTRACT
see report

15. SUBJECT TERMS

16. SECURITY CLASSIFICATION OF:			17. LIMITATION OF ABSTRACT	18. NUMBER OF PAGES	19a. NAME OF RESPONSIBLE PERSON
a. REPORT **unclassified**	b. ABSTRACT **unclassified**	c. THIS PAGE **unclassified**	**Same as Report (SAR)**	**65**	

Standard Form 298 (Rev. 8-98)
Prescribed by ANSI Std Z39-18

TABLE OF CONTENTS

LIST OF TABLES

LIST OF FIGURES

ABSTRACT

A factor of safety (FS) method for quantitative estimates of grid/time uncertainties for CFD solutions is derived to remove the deficiencies of GCI, corrected GCI_C, and correction factor (CF) methods, i.e., unreasonably small uncertainty when CF > 1 (estimated order of accuracy greater than theoretical) and lack of statistical analysis to prove 95% confidence for the estimated uncertainties to bound the true error. The approach follows the CF method but reflects the uncertainty instead of FS for CF < 1 for CF > 1 (CF = 1 is asymptotic range). FS at CF = 0 and 1 are determined by reliability and lower band of the confidence interval of the true mean based on statistical analysis using a large sample of analytical/numerical benchmarks covering 17 studies, 96 variables and 304 individual grid triplets. Only the FS method provides 95% confidence that the actual factor of safety FS_A > 1 for the 304 grid convergence studies: confidence intervals are 86.2%, 92.1%, 91.5%, and 95.7% for GCI, GCI_C, CF, and FS. For 20% of the data $1.1 \leq CF < 2.0$, GCI, GCI_C, and CF methods fail as only 47.4%, 71.2%, 72.9% confidence intervals are achieved, whereas 89.3% is achieved for the FS method. Only the FS method has 95% confidence the lower band of the confidence interval for FS_A is larger than 1.2 for different studies, variables, ranges of CF, and single CF values where multiple FS_A are available.

I. INTRODUCTION

Current quantitative error estimates for grid size and time convergence are based on Richardson extrapolation (RE), i.e. the error is expanded in a power series expansion with integer powers of grid spacing/time-step as a finite sum. It is common practice to retain only the 1st term of the series assuming the solutions are in the asymptotic range (AR), which leads to a grid triplet study. The grid convergence index (GCI) derived by Roache [1] can be used to estimate the uncertainties due to grid/time errors and is widely used and recommended by ASME [2] and AIAA [3]. Stern et al. derived the correction factor (CF) method [4] with improvements made by Wilson et al. [5]. They introduced a variable factor of safety (FS) as a function of the CF so that FS increases linearly with distance of solutions from the AR. CF is defined by:

$$CF = \frac{r^{p_{RE}} - 1}{r^{p_{th}} - 1} \tag{1}$$

where p_{RE} is the estimated order of accuracy and p_{th} is the theoretical order of accuracy. CF provides an important metric that quantifies the distance of solutions to the AR. As shown later, CF is also useful for statistical analysis, for which analytical benchmark (AB) or numerical benchmark (NB) data can be organized according to the same CF values. The CF method is validated for CF < 1 using AB including one-dimensional wave and two-dimensional Laplace equations. Since the AB approach AR from CF < 1, it is assumed that the FS for CF > 1 is obtained by reflecting the FS for CF < 1 with respect to AR (CF = 1) assuming FS is the same at the same distance from the AR.

There are several problems of using RE. As shown by Stern et al. [6], it is difficult to improve the accuracy by retaining more terms in the power series. When solutions are not in the AR, multiple grid triplet studies often show non-smooth convergence, i.e., p_{RE} approaches p_{th} in an oscillatory fashion with a large range of values [2]. RE requires at least 3 systematic high quality grids, which may be too expensive for industrial applications. The grid refinement ratio r must be carefully selected. r cannot be too large as the grids may resolve different flow physics. Too small values of r (i.e., very close to one) are also undesirable since solution changes will be

small and sensitivity to grid/time-step may be difficult to identify compared to iterative errors.

The non-smooth grid convergence problem may be resolved using the least square method (LSM) [7] or response surface method (RSM) [8], which requires at least 4 solutions. There are some issues of implementing the LSM/RSM: (1) the relationship between the LSM/RSM and the individual grid triplet studies is not established; (2) it does not discriminate between converging and diverging grid studies and the use of diverging solutions is not well founded; (3) the requirement of at least four gird solutions is often too expensive for industrial applications; (4) all solutions are required to be in the AR, which is contradictory to the use of non-smooth and non-monotonic converged solutions; and (5) it introduces additional uncertainties due to the least-square fit. The expensive cost of using RE may be resolved using the single-grid uncertainty estimate approach [9] but this approach is not well developed for three-dimensional problems and does not provide sensitivity of solutions to grid size and time step.

GCI and CF methods have two deficiencies. Uncertainty estimates when $p_{RE} > p_{th}$ (CF > 1) are unreasonably small in comparison to those with the same distance to AR for CF < 1. This is due to the fact that the error estimate δ_{RE} for the former is much smaller than that of the latter. There is no statistical evidence for what confidence interval GCI and CF can actually achieve. It is claimed by Roache [1] and the ASME performance test codes committee PTC 61 [10] that a 95% confidence interval is achieved for GCI with FS = 1.25 based on over 500 demonstrated cases by dozens of groups. However, this is only based on anecdotal observations as no statistical distributions or analysis are reported in the references cited in [1], [10], or [11] to support this claim.

A recent study by Logan and Nitta [8] evaluated 10 different methods on uncertainty estimates using limited statistical analysis including solution verification method reliability R_{sm} and the reduced Chi-Square X_{v*}^2. A higher value of X_{v*}^2 indicates that a solution verification method is too conservative. The use of corrected GCI (GCI$_C$) with FS = 1.25 is much closer to a 68% confidence estimate than 95%. There is no apparent correlation between R_{sm} and X_{v*}^2, i.e., a method may have very good R_{sm} but

2

$X_{v*}^2 >> 1$. Since this study only has 3 structure problems with 18 individual grid solutions, it was suggested that a larger sample set with the number of grid convergence sets much larger than 100 is needed to draw any general conclusions.

Two other recent studies [12, 13] have considered the use of different uncertainty estimates for different ranges of p_{RE} for monotonically converged solutions. The idea is not new as it was the basis for the CF method as per Stern et al. [4], although the CF method was not referenced. Eca and Hoekstra [12] extended the LSM for a nominally second-order accurate method, i.e., $0 < p_{RE} < 0.95$ ($0 < CF < 0.31$), $0.95 \leq p_{RE} < 2.05$ ($0.31 \leq CF < 1.05$), and $p_{RE} \geq 2.05$ ($CF \geq 1.05$). According to the authors, the estimates were based on the experience obtained in a variety of test cases and the suggestions and comments of the first Workshop on CFD Uncertainty Analysis [14]. Similar ideas were used by Rumsey and Thomas [13] who provided different formulas for different ranges of p_{RE} for a nominally third-order accurate method, i.e., $0 < p_{RE} < 0.95$ ($0 < CF < 0.13$), $0.95 \leq p_{RE} < 3.05$ ($0.31 \leq CF < 1.04$), and $p_{RE} \geq 3.05$ ($CF \geq 1.04$). Since the authors did not provide detailed derivation or validation of their estimates and p_{RE} ranges it is difficult to understand their differences. Here again statistical distributions or analysis are not reported.

The overall objective of this study is to develop a FS method that removes the above deficiencies and achieves an overall 95% confidence interval for the estimated uncertainty to bound the true error. The approach is to extend the CF method by reflecting uncertainty not FS for CF < 1 for CF > 1 with respect to the AR. The FS method provides the flexibility of specifying FS at CF = 0 and CF = 1, i.e., FS_0 and FS_1, which will be determined using rigorous verification studies covering a wide range of problems that have either AB or NB data. Statistical analysis includes the reliability and confidence interval for the mean of the actual factor of safety (FS_A). The FS method will be compared with GCI, GCI_C, and CF methods. It should be noted that the idea of reflecting uncertainty not FS for CF < 1 for CF > 1 with respect to the AR is not new as it was first reported in an earlier study by the authors [15]. However, the original idea was developed only logically based on observations that uncertainty estimates for CF > 1 are

unreasonably small and simply tested on one example of ship hydrodynamics application. It was not validated by AB and NB as conducted herein. Additionally, the original idea is altered so that users can flexibly specify FS_0 and FS_1. Due to these facts, the present work supersedes the previous report [15].

II. ERROR AND UNCERTAINTY ESTIMATE USING RICHARDSON EXTRAPOLATION

Grid/time convergence studies are conducted with multiple solutions using systematically refined grid sizes or time steps. First r for grid/time is selected. As an example, if 3, 2, and 1 represent the coarse, medium, and fine grids with grid spacing Δx_3, Δx_2, and Δx_1, respectively, then

$$r = \frac{\Delta x_2}{\Delta x_1} = \frac{\Delta x_3}{\Delta x_2} \tag{2}$$

Constant r is not required [1] but simplifies the analysis and thus used herein. Solution changes ε for medium-fine and coarse-medium solutions and the convergence ratio R are defined by

$$\begin{aligned} \varepsilon_{21} &= S_2 - S_1 \\ \varepsilon_{32} &= S_3 - S_2 \\ R &= \varepsilon_{21}/\varepsilon_{32} \end{aligned} \tag{3}$$

When $0 < R < 1$ solution monotonic convergence is achieved and generalized RE is used to estimate order-of-accuracy p_{RE}, the error δ_{RE} and numerical benchmark S_C. The error is expanded in a power series expansion with integer powers of grid spacing/time-step as a finite sum. The accuracy of the estimates depends on how many terms are retained in the expansion, the magnitude (importance) of the higher-order terms, and the validity of the assumptions made in RE theory. In general, $2n+1$ solutions are required to estimate S_C and the first n terms in the power expansion. When solutions are close to the AR, grid spacing is sufficient small and the lower-order terms in the expansion dominate. If only the first term is retained ($n=1$), three grid solutions are needed to provide estimates for p_{RE}, δ_{RE}, S_C

4

$$p_{RE} = \frac{\ln(\varepsilon_{32}/\varepsilon_{21})}{\ln(r)} \qquad (4)$$

$$\delta_{RE} = \frac{\varepsilon_{21}}{r^{p_{RE}} - 1} \qquad (5)$$

$$S_C = S_1 - \delta_{RE} \qquad (6)$$

Eqn. (5) provides the error estimate with both sign and magnitude but not an "error band" (uncertainty) in which the users can have some practical level of confidence.

Roache proposed the GCI method. The idea behind GCI is to approximately relate the ε_{21} in Eqn. (5) obtained by whatever grid convergence study (whatever p_{RE} and r) to the ε that would be expected from a grid convergence study of the same problem with the same fine grid using $p_{RE} = 2$ and $r = 2$, i.e. a grid doubling with a 2nd-order method. The relation is based on equality of the error estimates. Given an ε_{21} from an actual grid convergence test, the GCI is derived by calculating the error estimate δ_{RE} from Eqns. (5) and (4), then calculating an equivalent ε_{21} that would produce approximately the same δ_{RE} with $p_{RE} = 2$ and $r = 2$. The absolute value of that equivalent ε is the GCI for the fine grid solution, which is conveniently expressed as [1]

$$U_{GCI} = FS \frac{|\varepsilon_{21}|}{r^{p_{RE}} - 1} = FS \,|\,\delta_{RE}\,| \qquad (7)$$

FS can thus be regarded as a "factor of safety" over the RE error estimate δ_{RE}. Roache suggested FS = 1.25 for systematic grid-triplet studies using RE estimate for order of accuracy p_{RE} and FS = 3 for 2-grid sensitivity studies using theoretical estimate for order of accuracy p_{th}. In Fig. 1, FS = 1.25 is plotted versus CF, which suggests constant FS for all ranges of CF values.

Logan and Nitta [8] also used GCI$_C$, which modifies Eqn. (7) by discarding p_{RE} and use p_{th} when $p_{RE} > p_{th}$. As can be easily shown, GCI$_C$ is equivalent to multiply FS by CF when CF > 1, which leads to

$$U_{GCI} = \begin{cases} FS\left|\delta_{RE}\right| & CF \leq 1 \\ FS \times CF\left|\delta_{RE}\right| & CF > 1 \end{cases} \qquad (8)$$

The CF method was derived based on AB for CF < 1, which shows that an improved error estimate is to multiply Eqn. (5) by CF

$$CF\delta_{RE} = CF\left(\frac{\varepsilon_{21}}{r^{p_{RE}} - 1}\right) \tag{9}$$

The use of Eqn. (9) will replace p_{RE} using p_{th}. However, p_{RE} is not discarded but included in CF. The uncertainty is estimated by the sum of the absolute value of the corrected error estimate from RE and the absolute value of the amount of the correction

$$U = FS(CF)|\delta_{RE}| = |CF\delta_{RE}| + |(1 - CF)\delta_{RE}| \tag{10}$$

As criticized by Roache [16], Eqn. (10) is deficient for CF ≤ 1 in only providing 50% confidence level. Wilson et al. [5] revised Eqn. (10) for proper behavior for CF < 1 by increasing FS for decreasing CF, i.e. FS is a function of CF. Then the variable FS for CF < 1 is reflected for CF > 1 with respect to the AR (CF = 1). Additionally, they modified the formula for proper behavior for CF = 1 by providing 10% FS in the limit CF = 1 while smoothly merging with previous CF method uncertainty estimates for $|1 - CF| \geq 0.125$ for the uncorrected solutions.

$$U = FS(CF)|\delta_{RE}| = \begin{cases} \left[9.6(1 - CF)^2 + 1.1\right]|\delta_{RE}| & 0.875 < CF < 1.125 \\ \left[2|1 - CF| + 1\right]|\delta_{RE}| & 0 < CF \leq 0.875 \quad or \quad CF \geq 1.125 \end{cases} \tag{11}$$

As shown by Wilson et al. [5, 17] and Fig. 1, the CF method is equivalent to the GCI, but with a variable FS. The variable FS has the "common-sense" advantage in providing a quantitative metric to determine proximity of the solutions to the AR and approximately accounts for the effects of higher-order RE terms. The CF method has been used in ship hydrodynamics CFD workshops.

III. FACTOR OF SAFETY METHOD

The overall approach of the FS method follows the CF method [4, 5] with a linearly varying FS for CF < 1. However, it has two improvements on top of the CF method by introducing two flexible parameters, FS_0 and FS_1. Additionally, it reflects the uncertainty rather than the FS itself for CF <1 for CF > 1 with respect to the distance from CF = 1.

Recommended values of FS_0 and FS_1 are determined using large sample of AB or NB and statistical analysis compared to only AB and no statistical analysis for the CF method. The procedure is to minimize the two parameters until two criteria are met: (1) overall at least 95% confidence interval is achieved for the FS_A is larger than 1; (2) at least 95% confidence that the lower band of the confidence interval for the true mean FS_A is larger than 1.2.

Following Stern et al. [4] with improvements by Wilson et al. [5], the FS method first assumes that uncertainty estimate has the same form as Eqns. (10) and (11) for $CF \leq 1$, i.e. $U = FS(CF)\left|\delta_{RE}\right|$ and FS is a linear function of CF that increases with the distance from CF = 1. However, FS_1 and FS_0 are multiplied before the corrected estimate from RE and the absolute value of the amount of the correction, respectively:

$$U = FS_1 \,|\, CF\delta_{RE} \,| + FS_0 \,|\, (1-CF)\delta_{RE} \,| \tag{12}$$

Or

$$U = \underbrace{\left[FS_1 \,|\, CF \,| + FS_0 \,|\, 1-CF \,| \right]}_{FS(CF)} |\, \delta_{RE} \,| \tag{13}$$

For $0 < CF \leq 1$, the above formula becomes

$$U = \left[FS_1 CF + FS_0 (1-CF) \right] |\, \delta_{RE} \,| \qquad 0 < CF \leq 1 \tag{14}$$

To overcome the too small uncertainty estimate for $CF > 1$, the uncertainty instead of the FS in $CF \leq 1$ is reflected for $CF > 1$ with respect to the distance from the AR [15]. First, $r^{P_{RE}}$ in Eqn. (5) is re-expressed based on the definition of CF:

$$r^{P_{RE}} = CF \left(r^{P_{th}} - 1 \right) + 1 \tag{15}$$

Second, Eqn. (5) is substituted into Eqn. (14) with the use of Eqn. (15), which results in an alternative form of U

$$U = \left[FS_1 CF + FS_0 (1-CF) \right] \left| \frac{\varepsilon_{21}}{CF \left(r^{P_{th}} - 1 \right)} \right| \qquad 0 < CF \leq 1 \tag{16}$$

CF in the above equation is replaced by $2-CF$. Thus for the same r, p_{th}, and ε_{21}, Equation (16) becomes:

$$U = \frac{CF}{2-CF}\left[FS_1(2-CF)+FS_0(CF-1)\right]\left|\delta_{RE}\right| \qquad 1 < CF < 2 \qquad (17)$$

In summary, uncertainty for uncorrected solutions using the FS method is:

$$U = \begin{cases} \left[FS_1 CF + FS_0(1-CF)\right]|\delta_{RE}| & 0 < CF \leq 1 \\ \dfrac{CF}{2-CF}\left[FS_1(2-CF)+FS_0(CF-1)\right]\left|\delta_{RE}\right| & 1 < CF < 2 \end{cases} \qquad (18)$$

Compared to the CF method, the FS method introduces an additional term $CF/(2-CF)$ to compute U for CF > 1. When CF increases from 1 to 2, this term increases rapidly from 1 to infinity, which amplifies *FS* when solutions are further away from the AR. The FS method is only applicable for 0 < CF < 2. CF = 0 is the border of convergence and divergence such that grid errors/uncertainties are infinite due to infinite δ_{RE} as a result of $p_{RE} = 0$, i.e. solution changes for the medium and fine grids are equal to those for the coarse and medium grids. For CF > 2, solutions are too far from the AR and also regarded as divergent. Figure 1 compares the theoretical *FS* predicted by GCI, GCI$_C$, CF, and FS methods. FS = 1.0 suggests that the design meets but does not exceed the minimum requirements with no room for variation nor error while too high FS results in excessive weight and/or cost.

The FS method provides users flexibility in specifying FS$_0$ and FS$_1$. To determine the "optimal" values for FS$_0$ and FS$_1$ and validate the FS method requires "iterations" based on statistical analysis of a large sample of data (see Section 4). The iterations outcome are FS$_0$ = 2 and FS$_1$ = 1.25:

$$U = \begin{cases} (2-0.75CF)|\delta_{RE}| & 0 < CF \leq 1 \\ \dfrac{CF(0.5+0.75CF)}{2-CF}\left|\delta_{RE}\right| & 1 < CF < 2 \end{cases} \qquad (19)$$
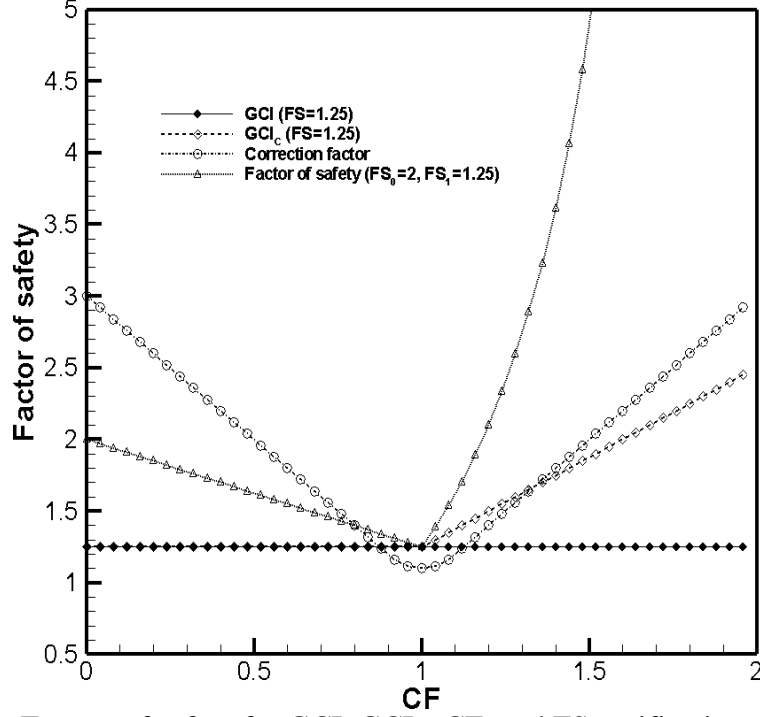
Figure 1. Factors of safety for GCI, GCI_C, CF, and FS verification methods.

IV. STATISTICAL ANALYSIS

Reliability R^1 is defined as

$$R = \frac{number \quad of \quad studies \quad FS_A > 1}{Total \quad number \quad of \quad studies} \tag{20}$$

where FS_A is defined as the ratio of the uncertainty estimate and the true error E_1 between the fine grid solution and the AB/NB solution S_C:

$$FS_A = \frac{U}{E_1} \tag{21}$$

$$E_1 = \left| \frac{S_1 - S_C}{S_C} \right| \tag{22}$$

R_{sm}=1-|Estimated fraction for $FS_A>1$ – Expected fraction for $FS_A >1$| used in [8] is deficient as it does not discriminate estimated fractions with the same distance below or

---

[1] R hereinafter not to be confused with R used before for convergence ratio

above the expected fraction (e.g., 91% estimated fraction inside has the same R_{sm} as 99% estimated fraction inside).

The confidence of mean analysis is based on the methodology and procedures summarized in [18]. If $X_i \, (i = 1, N)$ is any individual sample population/distribution, the sample mean of X_i is

$$\overline{X} = \frac{1}{N} \sum_{i=1}^{N} X_i \tag{23}$$

where N is the sample size. The standard deviation of the sample is defined by

$$S_{X_i} = \sqrt{\frac{\sum_{i=1}^{N} \left(X_i - \overline{X} \right)^2}{N-1}} \tag{24}$$

and is related to the standard deviation for the mean $S_{\overline{X}}$ by

$$S_{\overline{X}} = \frac{S_{X_i}}{\sqrt{N}} \tag{25}$$

To account for the effect of small number of the sampling data, student t-distribution is applied where the confidence interval for the mean is defined as:

$$k = t S_{\overline{X}} = \frac{t S_{X_i}}{\sqrt{N}} \tag{26}$$

The confidence interval of mean is that at least 95% confidence that true mean μ is bounded by $\overline{X} - k$ and $\overline{X} + k$

$$P\left(\overline{X} - k \leq \mu \leq \overline{X} + k \right) \geq 0.95 \tag{27}$$

The "outliers" for all the statistical analysis are identified using the Peirce's Criterion as summarized in [19]. Compared to the Chauvenet's criterion, Peirce's criterion is more rigorous, does not make an arbitrary assumption concerning the rejection of data, and theoretically accounts for the case where there is more than one suspect data.

The sample populations are constructed based on statistical analysis of AB and NB selected from 17 different studies covering 9 fluids, 5 thermal and 3 structure problems with additional information summarized in Table 1. The 17 studies were solved

Table 1. Verification studies

#	Case	Conditions	Verification variables	Grids	Outlier	AB/NB
1	1D[£] wave [6]	-	Wave profile	10 grids	0	AB
2	2D Laplace [5,7]	-	Arbitrary function	6 grids	0	AB
3	2D driven cavity [20]	Re=1000	Maximum/minimum Of stream-function, vorticity	4 grids	1	NB [21]
4	2D natural convection flows in square cavities [22]	Ra=10^4	Max. or monitored Velocity, location, temperature, and Nu	5 grids	2	NB
5	2D natural convection flows in square cavities [22]	Ra=10^5	Max. or monitored Velocity, location, temperature, and Nu	6 grids	1	NB
6	2D natural convection flows in square cavities [22]	Ra=10^6	Max. or monitored Velocity, location, temperature, and Nu	7 grids	0	NB
7	Backward-facing step [23]	Re=1.5×10^5	Reattachment length, velocity	7 grids	1	NB [24, 25]
8	2D driven cavity [26, 27]	Re=100	Velocity	5 grids	0	NB
9	2D driven cavity [26, 27]	Re=1000	Velocity	5 grids	0	NB
10	3D cubic cavity [26, 27]	Re=100	Velocity	4 grids	3	NB
11	Axisymmetric turbulent flow through a valve [28, 29]	Re=10^5	Velocity, TKE, ε	5 grids	4	NB
12	1D steady-state convection-diffusion [11]	Pe=1 and Pe=10	Arbitrary function	6 grids	0	AB
13	Isothermal cylinder enclosed by a square duct [27, 28, 29]	Ra=10^6, Pr=10	Velocity, temperature	5 grids	1	NB
14	Premixed methane/air laminar flat flame on a perforated burner [28, 30, 31]	Inlet temperature 298.2K	Velocities, temperature	7 grids	2	NB
15	Data for "exact" grid convergence set [8]	contrived	-	7 grids	0	AB
16	Bean bending problem for 2nd series [8]	2nd series	Beam bending stress, Beam end deflection	7 grids with 5 systematically refined	3	AB
17	Beam bending problem for 3rd series [8]	3rd series	Beam bending stress, Beam end deflection	4 grids	0	AB

[£] D stands for "dimensional"

on four, five, or six refinement levels using a systematic grid refinement ratio 2 ($r=2$) for different kinds of flows, using different grids and different numerical schemes. The

17 studies constitute 96 variables (velocity, locations max/min, temperature, turbulent kinetic energy, stream function, beam bending stress, and beam end deflection) of which either one or multiple grid convergence studies are available, which gives a total of 304 individual monotonically converged grid studies. 304 grid studies have 304 CF values of which at least 5 FS_A are available at 16 different CF. Details about the numerical schemes, solver, and boundary conditions can be found in the corresponding references.

The statistical analysis is performed in different ways resulting in a total of 24 different distributions. For each distribution, variables R, $\overline{X}$, $S_{\overline{X}}$, and $\overline{X} - tS_{\overline{X}}$ are calculated. As summarized in Table 2, the 1st and 2nd distributions are for the 17 means of studies and the means of the 96 variables of the 17 studies, respectively. Then statistical analysis is conducted for different ranges of CF where an averaging process is performed using a tolerance $\Delta CF = 0.01$, i.e., CF values are regarded to be the same if the difference between two CF values is less than 0.01. A smaller value with $\Delta CF = 0.001$ is evaluated and no significant effects on the statistics are observed. After the averaging process, the 3rd to 8th distributions are analyzed for different ranges of CF values, i.e., (0-2), (0-0.4), (0.4-0.9), (0.9-1.1), (1.1-1.6), and (1.6-2.0), for which the results the summarized in Table 3. Table 4 shows the 9th to 24th distributions that are at the 16 CF values where there are more than 4 monotonic converged grid studies and thus more than 4 FS_A for each CF. The numbers of outliers for each study and the 16 CF where multiple FS_A (>4) are available are summarized in Table 1 and Table 4, respectively.

Table 2. Mean, standard deviation of the mean, and reliability excluding outliers based on different studies

Factor of safety	# points	Statistics	GCI	GCI$_C$	CF	FS	t
Means of studies	17	$\overline{X}$	1.61	1.72	2.27	3.25	1.75
		$S_{\overline{X}}$	0.16	0.16	0.31	0.81	
		$\overline{X} - tS_{\overline{X}}$	1.33	1.44	1.73	1.83	
		R (%)	82.35	94.12	94.12	94.12	
Means of all variables of 17 studies	96	$\overline{X}$	1.63	1.73	2.24	2.74	1.67
		$S_{\overline{X}}$	0.09	0.09	0.19	0.28	
		$\overline{X} - tS_{\overline{X}}$	1.48	1.58	1.92	2.27	
		R (%)	88.54	91.67	91.67	95.83	

Table 3. Mean, standard deviation of the mean, and reliability excluding outliers based on different ranges of correction factors using non-averaged factor of safety

CF	# points	Statistics	GCI	GCI$_C$	CF	FS	t
0–2	304	$\overline{X}$	1.69	1.76	2.34	2.60	1.65
		$S_{\overline{X}}$	0.11	0.11	0.27	0.24	
		$\overline{X}-tS_{\overline{X}}$	1.51	1.58	1.89	2.20	
		R (%)	86.18	92.11	91.45	95.72	
0–0.4	27 (8.88%)	$\overline{X}$	4.77	4.77	10.20	7.16	1.71
		$S_{\overline{X}}$	1.06	1.06	2.54	1.70	
		$\overline{X}-tS_{\overline{X}}$	2.96	2.96	5.86	4.25	
		R (%)	96.30	96.30	100	96.30	
0.4–0.9	96 (31.58%)	$\overline{X}$	1.74	1.74	2.24	2.06	1.67
		$S_{\overline{X}}$	0.08	0.08	0.14	0.11	
		$\overline{X}-tS_{\overline{X}}$	1.61	1.61	2.01	1.88	
		R (%)	93.75	93.75	95.83	95.83	
0.9–1.1	125 (41.11%)	$\overline{X}$	1.29	1.30	1.15	1.34	1.98
		$S_{\overline{X}}$	0.02	0.02	0.02	0.02	
		$\overline{X}-tS_{\overline{X}}$	1.25	1.26	1.11	1.30	
		R (%)	96.0	96.0	94.4	98.4	
1.1–1.6	48 (15.79%)	$\overline{X}$	1.02	1.29	1.24	2.16	1.68
		$S_{\overline{X}}$	0.06	0.07	0.07	0.15	
		$\overline{X}-tS_{\overline{X}}$	0.92	1.17	1.12	1.91	
		R (%)	47.92	77.08	70.83	87.5	
1.6–2.0	8 (2.63%)	$\overline{X}$	0.97	1.74	2.01	16.09	1.90
		$S_{\overline{X}}$	0.14	0.25	0.29	3.80	
		$\overline{X}-tS_{\overline{X}}$	0.70	1.27	1.46	8.87	
		R (%)	37.5	37.5	87.5	100	

Table 4. Statistics excluding outliers at 16 different correction factors

CF	# points	#outliers	Statistics	GCI	GCI$_C$	CF	FS	t
0.625	4	1	$\overline{X}$	1.69	1.69	2.36	2.07	2.35
			$S_{\overline{X}}$	0.09	0.09	0.12	0.11	
			$\overline{X}-tS_{\overline{X}}$	1.48	1.48	2.07	1.81	
			R (%)	100	100	100	100	
0.675	9	0	$\overline{X}$	1.90	1.90	2.51	2.27	1.86
			$S_{\overline{X}}$	0.12	0.12	0.15	0.14	
			$\overline{X}-tS_{\overline{X}}$	1.69	1.69	2.23	2.02	
			R (%)	100	100	100	100	

0.745	7	2	$\overline{X}$	1.60	1.60	1.94	1.85	1.94
			$S_{\overline{X}}$	0.058	0.058	0.070	0.067	
			$\overline{X} - tS_{\overline{X}}$	1.49	1.49	1.80	1.72	
			R (%)	100	100	100	100	
0.825	14	0	$\overline{X}$	1.59	1.59	1.71	1.75	1.77
			$S_{\overline{X}}$	0.104	0.104	0.111	0.114	
			$\overline{X} - tS_{\overline{X}}$	1.40	1.40	1.51	1.55	
			R (%)	100	100	100	100	
0.865	12	1	$\overline{X}$	1.48	1.48	1.50	1.60	1.80
			$S_{\overline{X}}$	0.114	0.114	0.116	0.123	
			$\overline{X} - tS_{\overline{X}}$	1.28	1.28	1.29	1.38	
			R (%)	100	100	100	100	
0.895	4	1	$\overline{X}$	1.37	1.37	1.33	1.46	2.35
			$S_{\overline{X}}$	0.015	0.015	0.019	0.018	
			$\overline{X} - tS_{\overline{X}}$	1.33	1.33	1.28	1.42	
			R (%)	100	100	100	100	
0.915	9	1	$\overline{X}$	1.36	1.36	1.28	1.43	1.86
			$S_{\overline{X}}$	0.102	0.102	0.096	0.107	
			$\overline{X} - tS_{\overline{X}}$	1.17	1.17	1.10	1.23	
			R (%)	71.4	71.4	71.4	100	
0.945	7	1	$\overline{X}$	1.33	1.33	1.20	1.38	1.94
			$S_{\overline{X}}$	0.007	0.007	0.006	0.007	
			$\overline{X} - tS_{\overline{X}}$	1.32	1.32	1.19	1.36	
			R (%)	100	100	100	100	
0.955	4	1	$\overline{X}$	1.33	1.33	1.19	1.36	2.35
			$S_{\overline{X}}$	0.003	0.003	0.002	0.003	
			$\overline{X} - tS_{\overline{X}}$	1.32	1.32	1.19	1.36	
			R (%)	100	100	100	100	
0.965	7	1	$\overline{X}$	1.28	1.28	1.14	1.31	1.94
			$S_{\overline{X}}$	0.006	0.006	0.006	0.006	
			$\overline{X} - tS_{\overline{X}}$	1.27	1.27	1.13	1.30	
			R (%)	100	100	100	100	
0.985	7	1	$\overline{X}$	1.27	1.27	1.12	1.28	1.94
			$S_{\overline{X}}$	0.013	0.013	0.011	0.013	
			$\overline{X} - tS_{\overline{X}}$	1.24	1.24	1.09	1.25	
			R (%)	100	100	100	100	

1.005	50	5	$\overline{X}$	1.26	1.27	1.11	1.27	1.68
			$S_{\overline{X}}$	0.025	0.025	0.022	0.025	
			$\overline{X}-tS_{\overline{X}}$	1.22	1.22	1.08	1.23	
			R (%)	96	96	94	96	
1.015	6	0	$\overline{X}$	1.24	1.26	1.09	1.29	2.02
			$S_{\overline{X}}$	0.008	0.008	0.007	0.010	
			$\overline{X}-tS_{\overline{X}}$	1.23	1.24	1.08	1.27	
			R (%)	100	100	100	100	
1.095	5	0	$\overline{X}$	1.72	1.89	1.64	2.21	2.13
			$S_{\overline{X}}$	0.17	0.19	0.16	0.22	
			$\overline{X}-tS_{\overline{X}}$	1.36	1.49	1.30	1.75	
			R (%)	100	100	100	100	
1.145	13	1	$\overline{X}$	1.19	1.36	1.23	1.73	1.78
			$S_{\overline{X}}$	0.11	0.12	0.11	0.15	
			$\overline{X}-tS_{\overline{X}}$	1.00	1.15	1.03	1.45	
			R (%)	69.23	76.92	69.23	92.31	
1.295	8	2	$\overline{X}$	1.09	1.42	1.39	2.37	1.90
			$S_{\overline{X}}$	0.05	0.06	0.06	0.11	
			$\overline{X}-tS_{\overline{X}}$	1.00	1.29	1.27	2.17	
			R (%)	75	100	100	100	

Determination of the optimal values for FS_0 and FS_1 require iterations since computation of the mean, standard deviation, and k require the values of FS_0 and FS_1 known as a priori. Two criteria are used to determine if the selected values are acceptable. The first criterion is that for the total 304 grid convergence studies at least 95% confidence is achieved for $FS_A > 1$, i.e.,

$$R > 95\% \tag{28}$$

R is also used to estimate the performance of different verification methods for different studies, different regions of CF values, and at the 16 different CF values with multiple solutions. The 2nd criterion is that there will be at least 95% confidence that the lower band of the confidence interval for the mean FS_A is larger than $FS_{A,min}$. The appropriate values of $FS_{A,min}$ are often determined based on risks/reliability, accuracy, and cost, etc. and show a large variations from 1.2 to 5 for different practical applications. For example, 1.2 is used for new bridges and road marks, 3.0 is used for automobiles, and 3.5

to 4.0 are used for pressure vessels, etc. $FS_{A,min}$ is thus chosen to be 1.2 in this study

$$P\left(1.2 \leq \overline{X} - k \leq \mu \leq \overline{X} + k\right) \geq 0.95 \qquad (29)$$

It is obvious that when Eqn. (29) is satisfied

$$P\left(\overline{X} \geq 1.2\right) \geq 0.95 \qquad (30)$$

$$P\left(\mu \geq 1.2\right) \geq 0.95 \qquad (31)$$

When the two criteria are met, a minimum set of values are accepted. In this study, ($FS_0 =$ 3, $FS_1 = 2$), ($FS_0 = 3$, $FS_1 = 1.5$), ($FS_0 = 2$, $FS_1 = 1.5$) and ($FS_0 = 2$, $FS_1 = 1.25$) are found to meet the two criteria. Since the first three sets of data are too conservative (i.e, provide too large FS_A), ($FS_0 = 2$, $FS_1 = 1.25$) is determined to be the recommended values, which are used and compared with GCI, GCI_C, and CF methods for the same sample of data to evaluate the mean, standard deviation for the mean, lower band value for the confidence interval of the mean FS_A, and the reliability based on different studies and different ranges of CF values.

It should be noted that statistical analysis is performed based on the following fact. The error and uncertainty estimates are systematic, but since the real error E_1 is random, the ratio between them (i.e., FS_A) is randomly distributed. In other words, it is assumed that there are no correlated biased errors between different studies. Since FS_A is randomly distributed, the confidence interval for the mean reveals how close $\overline{X}$ is to μ for FS_A.

V. ANALYTICAL AND NUMERICAL BENCHMARK DATA

All the 17 studies summarized in Table 1 used the same grid refinement ratio 2 to generate the grids systematically. For each study, solutions on multiple grids are extracted and convergence studies are performed for each variable. Only monotonically converged grid studies with $0 < CF < 2$ are used, which constitute about 90% of all the grid convergence studies. The other 10% with oscillatory convergence, monotonic divergence, and oscillatory divergence are discarded. p_{RE}, δ_{RE}, and S_C are evaluated using Eqns. (4), (5), and (6), respectively.

For each study, two types of figures are plotted and analyzed. To investigate the convergence characteristics of each variable, $|U|$, actual error $|E_1|$, and CF are graphed versus the ratio of grid spacing $\Delta x/\Delta x_{\text{finest}}$. Additionally, FS_A is plotted versus CF to show the actual behavior of each method for different ranges of CF values, which enables the evaluation of different methods on whether the uncertainty estimate bound the true error ($|U| > |E_1|$). Details of these figures and discussions are presented in Appendix 1.

37 of the 96 variables only have two grid triplet studies, which prohibit studies of the convergence characteristics of those variables. However, the errors do show decreasing values when the grids are refined. Of the remaining 59 variables that have multiple grid triplet studies, ideal convergence is only achieved for 6 of the variables such as the one-dimensional wave equation, i.e., errors predicted by the four methods monotonically decrease continuously as the solutions are approaching the AR when grids are refined. The other variables oscillatorially approach the AR when the grids are refined. FS_A of all variables for each study are also examined for different CF values, which will be discussed in more details in the next section.

VI. STATISTICAL ANALYSIS RESULTS

Figure 2 shows the FS_A without averaging and without excluding outliers using the four different methods for the total 304 verification studies. There are some cases at CF around 0.5, 0.65, 0.8, 1, and 1.4 that none of the methods achieves $FS_A > 1$. As shown later, some of these points are outliers but the rest of them are not. Compared to the CF method, GCI predicts a lower and higher FS_A near CF = 0 and CF = 1, respectively, which is consistent with the theoretical FS distribution shown in Figure 1. Compared to GCI, GCI_C predicts a little higher FS_A for CF > 1 but still not high enough to bound most of the errors. Both GCI and the CF methods do not provide sufficient large FS_A for CF > 1, which is corrected by the FS method as it shows a nearly "symmetric" distribution of FS_A respect to CF = 1.

Figure 3 shows FS_A with/without averaging using $\Delta CF = 0.01$ and $\overline{X} \pm tS_{\overline{X}}$ for CF where at least four FS_A are available excluding outliers using the four methods. At the CF where multiple FS_A are available, the number of sampled data from left to right: 4, 9,

7, 14, 12, 4, 9, 7, 4, 7, 7, 50, 6, 5, 13, 8 points. It is observed that the averaging itself only helps to remove a few "unbounded" points but still cannot drag all the FS_A to be larger than 1 for all the methods. For $\overline{X} - tS_{\overline{X}}$, GCI has $FS_A < 1$ for most $CF > 1$. GCI_C increases the FS_A magnitude for $CF > 1$ but still not large enough to be greater than 1.2 for all CF where multiple FS_A are available. Compared to GCI and GCI_C, CF predicts lower FS near $CF = 1$ and similar magnitude of FS for $CF > 1$. Only the FS method bounds the largest fraction of the error and provides a minimum $FS_A > 1.2$ for all CF where multiple FS_A are available.
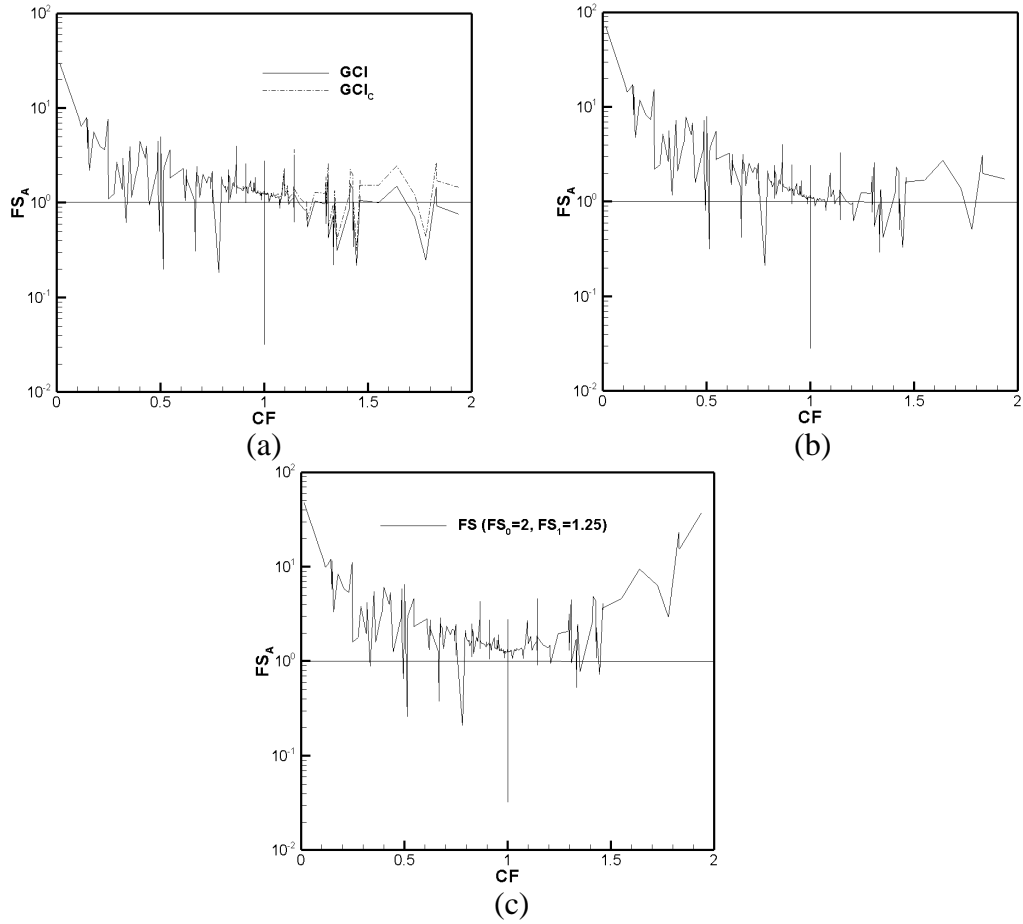
Figure 2 Actual factor of safety without averaging and without excluding outliers: (a) GCI and GCI_C, (b) CF method, (c) FS method.
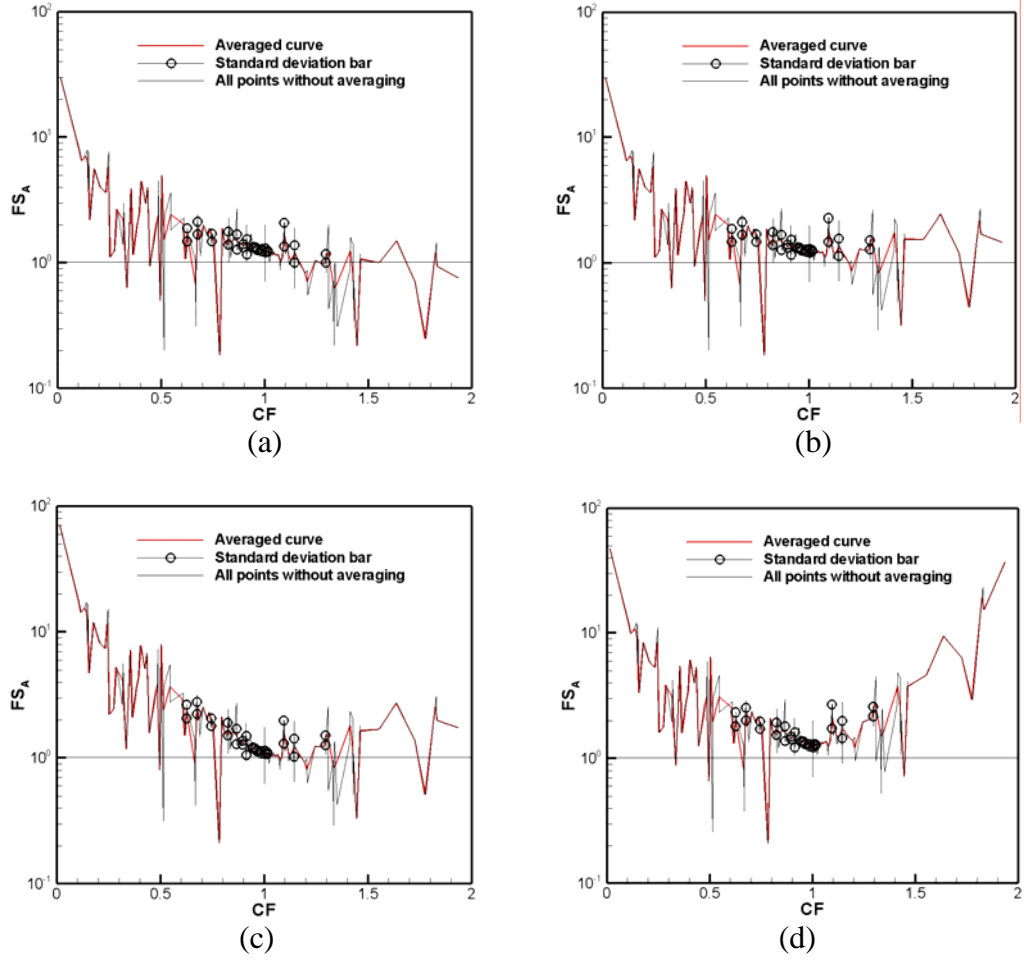
Figure 3 Actual factor of safety with/without averaging using $\Delta CF = 0.01$ and $\overline{X} \pm tS_{\overline{X}}$ for CF where multiple FS_A are available (number of sampled data from left to right: 4, 9, 7, 14, 12, 4, 9, 7, 4, 7, 7, 50, 6, 5, 13, 8 points, respectively) excluding outliers: (a) GCI, (b) GCI_C, (c) CF method, (d) FS method.

Figure 4 shows the standard deviation based on the mean ($S_{X_i}/\overline{X}$) for the different methods excluding outliers at the 16 CF where multiple FS_A are available. $S_{X_i}/\overline{X}$ is the same for different methods as dividing by the mean cancels the different factors of safety used in the formula. Overall $S_{X_i}/\overline{X}$ shows strong oscillations with magnitude decreasing when approaching the AR. This is consistent with the facts that

larger number of verification studies are available close to the AR than those far away from AR, which will lead to smaller S_{X_i}.
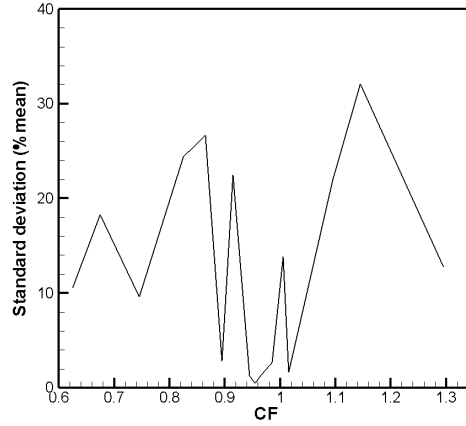
Figure 4 Standard deviation based on mean for different methods excluding outliers at the 16 CF where multiple FS$_A$ are available.

Tables 2 and 3 show the statistics for the four methods, either based on different studies and variables (Table 2) or based on different ranges of CF values (Table 3). The outliers have been removed. Based on 17 studies, none of the methods achieves 95% (R > 95%) likely due to the small population number. GCI has the smallest R = 82.4% while the other three methods have higher R = 94.1%. $\overline{X}$ of FS$_A$ for the 17 studies are increasing from 1.61 for GCI to 3.25 for FS. $S_{\overline{X}}$ is increasing from 0.16 for GCI to 0.81 for FS method. Based on all 96 variables considered, only the FS method has R > 95% while R for other methods are: R (GCI) < R (GCI$_C$) = R (CF) < R (FS). Compared to values using 17 studies, GCI, GCI$_C$, and CF methods show no significant changes of $\overline{X}$ but significant lower $S_{\overline{X}}$. $\overline{X}$ and $S_{\overline{X}}$ of the FS method decrease to 2.74 and 0.28, respectively. For all four methods, $\overline{X} - tS_{\overline{X}} > 1.2$ is met based on either the 17 studies or 96 variables.

FS$_A$ presented in Table 2 based on different studies and variables show larger mean FS$_A$ of FS method than any other method. This may be misleading as it seems that the higher reliability using the FS method is due to the larger FS. In fact, statistical analysis using different studies involves averaging of different verification studies that have $0 < CF < 2$. This will increase the overall mean significantly as the FS far away from the AR is much larger than FS close to the AR for the CF and FS methods. To

20

illustrate the distribution of FS_A and evaluate the effectiveness of different methods in different ranges of CF, Table 3 shows statistics for different ranges of CF using non-averaged FS_A excluding outliers. For the whole range of CF (0-2): only FS has R > 95% with R = 86.2% for GCI, R = 92.1% for GCI_C, 91.5% for CF, and 95.7% for FS methods. For 0 < CF < 0.9, all methods show R > 93%. However for 18% of the data (CF = 1.1-2.0), only 47.4%, 71.2%, 72.9% confidence interval can be achieved for GCI, GCI_C, and FS, respectively, while R = 89.3% for the FS method. For the range of CF (0-2), all the methods meet $\overline{X} - tS_{\overline{X}} > 1.2$. However, when the CF (0-2) is broken into different ranges, only FS method always satisfies $\overline{X} - tS_{\overline{X}} > 1.2$. For GCI, GCI_C, and CF methods, CF ranges where $\overline{X} - tS_{\overline{X}} < 1.2$ are (1.1-2.0) for GCI, (1.1-1.6) for GCI_C, and (0.9-1.6) for the CF method. This puts a very high risk of using the three methods on practical applications since many verification studies for complex geometries and high Reynolds number flows often approach the AR oscillatorily with the different sets of grids, which has been demonstrated in many previous simulations in CFD workshops and an example for ship hydrodynamics as provided in the next section. It should be also noted that different choices of ranges of CF values, for example 0-0.4, 0-0.8, 0.8-1.2, 1.2-1.6, and 1.6-2.0, only cause minor changes of the fraction bounded and the conclusions drawn above are general.

Table 4 additionally provides statistics for the 16 CF where at least 4 FS_A are available after removing the outliers. For the 11 CF that are less than 1, all methods have R = 100%. Near the AR where CF = 1.005, GCI, GCI_C, and FS have the same reliability R = 96%, which is larger than R = 94% for the CF method. For CF close to the AR but larger than 1 (CF = 1.015 and 1.095), R = 100% for all methods. However, at CF = 1.145, only R = 69.23% is achieved for GCI and CF methods, R = 76.92% for GCI_C method, but with 92.31% for the FS method. When solutions are far away from the asymptotic range (CF = 1.295), GCI only provides R = 75% while the other three methods can achieve R = 100%. When CF < 1, the mean FS_A $\overline{X}$ is the same for the GCI and GCI_C methods. For CF = 0.625, 0.675, and 0.745, $\overline{X}(GCI) = \overline{X}(GCI_c) < \overline{X}(FS) < \overline{X}(CF)$. For CF = 0.825 and 0.865, $\overline{X}(GCI) = \overline{X}(GCI_c) < \overline{X}(CF) < \overline{X}(FS)$. For CF = 0.895, 0.915, 0.945, 0.955, 0.965, and 0.985, $\overline{X}(CF) < \overline{X}(GCI) = \overline{X}(GCI_c) < \overline{X}(FS)$. For CF = 1.005, 1.015, and

21

1.095, $\overline{X}(CF) < \overline{X}(GCI) < \overline{X}(GCI_C) \le \overline{X}(FS)$. For CF = 1.145 and 1.295, $\overline{X}(GCI) < \overline{X}(CF) < \overline{X}(GCI_C) < \overline{X}(FS)$. The different magnitudes of $\overline{X}$ follow the theoretical values of FS at different CF as shown in Figure 1. Since a larger FS will result in a larger standard deviation, the $S_{\overline{X}}$ follow the correlations above for $\overline{X}$ at the same CF. FS is the only method that satisfies $\overline{X} - tS_{\overline{X}} > 1.2$ at all the 16 CF. $\overline{X} - tS_{\overline{X}} > 1.2$ is observed for GCI at CF = 0.915, 1.145, and 1.295; for GCI_C at CF = 0.915, and 1.145; and for CF at CF = 0.915, 0.945, 0.955, 0.965, 0.985, 1.005, 1.015 and 1.145. This indicates that the GCI and GCIC don't have sufficient FS far away from the asymptotic range for CF > 1, whereas CF method does not provide enough FS close to the AR.

VII. EXAMPLE FOR SHIP HYDRODYNAMICS APPLICATIONS

To evaluate the behaviors of the four methods for practical applications, they are applied for a recent study [32] that used computational towing tank procedures for single run curves of resistance and propulsion for the high-speed transom ship Athena barehull with a skeg using the general-purpose solver CFDShip-Iowa-V.4 [33]. In this study, Xing et al. investigated the issue of achieving the AR by continuously refining the grid from the coarsest grid (grid 7 with 360,528 points) to the finest grid (grid 1 with 8.1 million points) for the Athena bare hull with skeg with 2 degrees of freedom (pitch and heave) at Froude number (Fr) 0.48. The grids are designed with a systematic grid refinement ratio $r = 2^{0.25}$, which allows 9 sets of grids for verification and validation (V&V) with 5 sets with $r = 2^{0.25}$ (5, 6, 7; 4, 5, 6; 3, 4, 5; 2, 3, 4; and 1, 2, 3), 3 sets with $r = 2^{0.5}$ (3, 5, 7; 2, 4, 6; and 1, 3, 5), and 1 set with $r = 2^{0.75}$ (1,4,7). The distribution of iterative errors $0.1S_{fine} \le U_I \le 0.3S_{fine}$ for grids 1 to 7 is shown in Figure 5(b) and 5(d) for resistance coefficients and motions, respectively. U_I is of the same order of magnitude for all the grids, which suggests that it is mainly determined by the iterative method applied and independent of grid resolutions. As shown in Table 5, C_{TX} monotonically converges for grids (2, 4, 6), (1, 3, 5), (4, 5, 6), (3, 4, 5), (2, 3, 4), and (1, 2, 3), of which grids (1, 2, 3) have the smallest grid uncertainty and grids (3, 4, 5) are closest to the AR based on CF closest to one. C_{TX} oscillatorily diverges on grids (5, 6, 7), and monotonically diverges

on grids (3, 5, 7) and (1, 4, 7). All the diverged solutions involve the coarsest grid 7, which is likely due to the insufficient resolution of the coarsest grid 7. As shown in Figure 5(a), C_{TX} for grid 7 does not follow the trend as shown for grids 6-1. Figure 5(a) also shows frictional and pressure resistance coefficients C_{fX} and C_{PX} on all the grids. Figure 5(b) shows the magnitudes of the relative changes of solutions ε_N between two successive grids with respect to the solutions on the finest grid 1. When grids are refined from 5 to 1, ε_N systematically decreases for C_{TX} and C_{fX} while oscillatory decreases for C_{PX}. U_G for grids (4, 5, 6) is unreasonable large as it is too far away from the AR. U_G for grid studies (2, 3, 4) and (1, 2, 3) using GCI, GCI_C, and CF are unreasonable small due to

Table 5. Verification study for C_{TX} of Athena bare hull with skeg (*Fr*=0.48)[*].

Grids	r	R_G	P_G	CF	U_G (%)			
					GCI	GCI_C	CF	FS
2, 4, 6	$2^{0.5}$	0.63	1.32	0.58	3.34	3.34	4.90	4.17
1, 3, 5	$2^{0.5}$	0.40	2.66	1.51	**0.72**	**1.09**	**1.16**	**2.90**
4, 5, 6	$2^{0.25}$	0.97	0.16	0.07	52.7	52.7	125.2	85.2
3, 4, 5	$2^{0.25}$	0.80	1.27	0.59	4.98	4.98	7.23	6.20
2, 3, 4	$2^{0.25}$	0.60	2.98	1.64	**1.07**	**1.75**	**1.95**	**6.64**
1, 2, 3	$2^{0.25}$	0.50	4.00	2.42	0.58	1.40	1.11	-

[*]U_G is %S_{fine}; C_{TX} is based on static wetted area;

Table 6. Verification study for motions of Athena bare hull with skeg (*Fr*=0.48)*

Parameter	Grids	r	R_G	P_G	CF	U_G (%)			
						GCI	GCI_C	CF	FS
Sinkage	1, 3, 5	$2^{0.5}$	0.31	3.4	2.25	0.64	1.44	1.8	-
Sinkage	2, 3, 4	$2^{0.25}$	0.13	12	16.92	0.05	0.88	1.37	-
Trim	1, 3, 5	$2^{0.5}$	0.48	2.13	1.09	**4.12**	**4.49**	**3.89**	**5.21**
Trim	4, 5, 6	$2^{0.25}$	0.86	0.89	0.40	24.42	24.42	42.87	33.17
Trim	2, 3, 4	$2^{0.25}$	0.53	3.69	2.16	3.35	7.25	8.92	-
Trim	1, 2, 3	$2^{0.25}$	0.53	3.71	2.18	1.73	3.77	4.64	-

*U_G is %S_{fine}
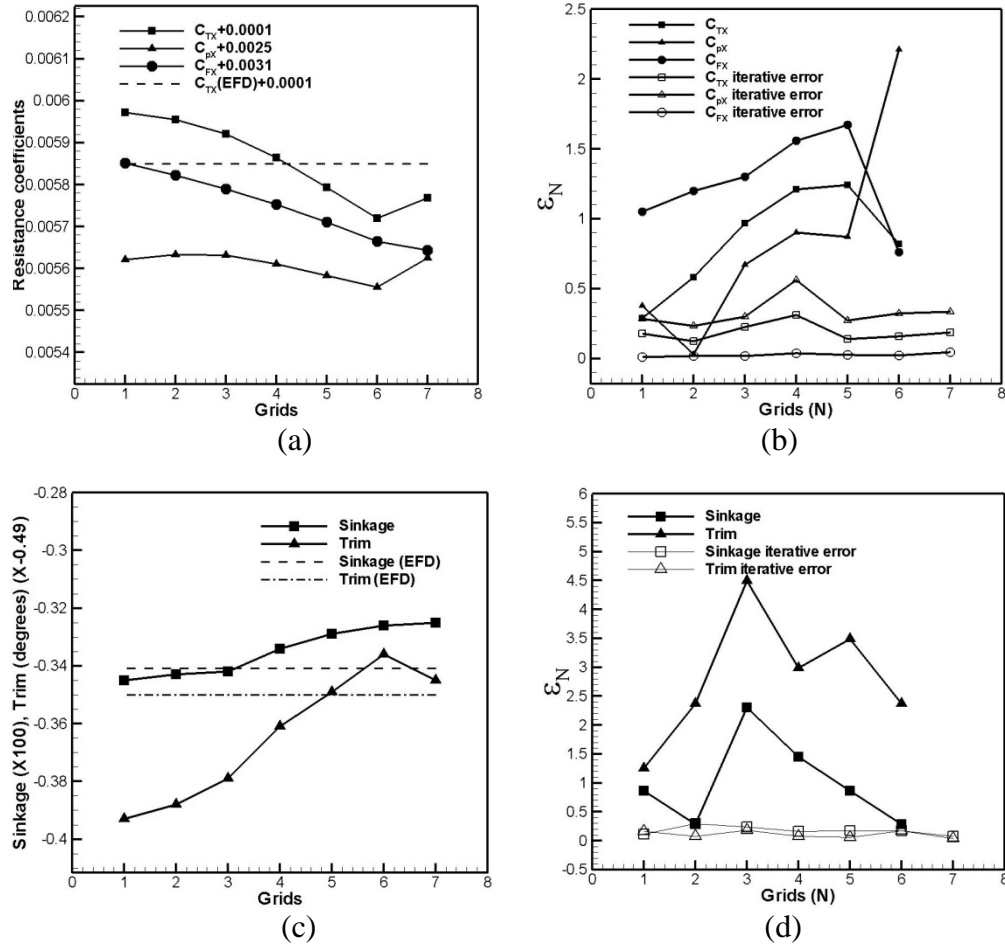
Figure 5. Verification for resistance and motions for Athena bare hull with skeg
(Fr=0.48): (a) resistance coefficients, (b) relative change $\varepsilon_N = \left|\left(S_{N-1} - S_N\right)/S_1\right| \times 100$
and iterative errors for resistance coefficients, (c) sinkage and trim, (d) relative
change ε_N and iterative errors for sinkage and trim.

the deficiency discussed before while U_G of the FS method for these two studies are more
reasonable on (2, 3, 4) but unfortunately invalid for (1, 2, 3) due to CF > 2 caused by the
contamination of the iterative error on the fine grid. As shown by Figure 5(b), separating
iterative errors from grid uncertainties is problematic for the finer grids since iterative
and grid uncertainties are of the same order of magnitude. Implementation of more
accurate and efficient iterative methods to speed up the convergence (e.g., multigrid) will
be necessary. However, ε_N of the current study does show systematic decreasing for C_{TX}
and C_{fX} and oscillatory decreasing for C_{PX}. C_{TX}, C_{fX}, and C_{PX} show different rates of

approaching the AR. Table 6 shows that motions are more difficult to converge than resistance coefficients. Monotonic converged solutions are achieved only for trim on grids (1, 3, 5) and (4, 5, 6). For trim on grids (1, 3, 5), FS method again predicts more reasonable U_G than the other three methods. For trim on grids (4, 5, 6), FS method also predicts larger U_G than GCI and GCIC methods but lower U_G than the CF method that seems to be too conservative at CF = 0.4.

VIII. CONCLUSIONS

A factor of safety method for quantitative estimates of grid and time-step convergence uncertainties for CFD solutions is derived to remove the two deficiencies of using GCI, GCI_C, and CF methods, i.e., unreasonably small uncertainty when CF > 1 and lack of statistical analysis to prove 95% confidence for the estimated uncertainties to bound the true error. The approach follows the CF method but by reflecting uncertainty instead of FS for CF < 1 for CF > 1 with respect to the AR (CF = 1). Additionally, the FS method provides flexibility for factors of safety at CF = 0 and CF = 1, which are determined by the overall reliability of the method and lower band of the confidence interval of the true mean based on statistical analysis. The statistical analysis is based on a large sample of AB and NB covering 17 studies with 96 variables and 304 individual grid triplet studies, as well as one practical application in ship hydrodynamics. Results showed that FS method is the only one that provides at least 95% confidence that the uncertainty estimate will bound the true error (FS_A > 1) for the 304 grid convergence studies, i.e., confidence intervals are 86.2%, 92.1%, 91.5%, and 95.7% for the GCI, GCI_C, CF, and the FS methods, respectively. For 20% of the selected data when $1.1 \leq$ CF < 2.0, GCI, GCI_C, and CF fail as only 47.4%, 71.2%, 72.9% confidence interval can be achieved for them, respectively, while 89.3% is achieved for the FS method. The FS method is also the only one that has at least 95% confidence the lower band of the confidence interval for the true mean FS_A is larger than 1.2 for different studies, different variables, different ranges of CF, and different single CF values where multiple FS_A are available.

Although a large sample of populations with either analytical or numerical benchmark data have been used, additional rigorous verification studies (AB/NB or

25

industrial applications) are needed to further validate the recommended FS_0 and FS_1, especially those demonstrating that the AR is achieved when grids are refined. This has two benefits: (1) reduced S_{X_i} and thus k, which will likely provide a "converged curve" for the factor of safety for different CF; (2) enabled Chi-square analysis for evaluation of confidence interval for $S_{\overline{X}}$. Further evaluation of the LSM is needed especially using statistical analysis tools in this study. There are other unresolved issues and complex factors such as mixed numerical schemes, coupled numerical and modeling errors for large eddy simulation and detached eddy simulation and single-grid estimator. Even though only a small fraction (5.6%) of data is outliers, it is worthy investigating why.

References

[1] Roache, P.J., 1998, "Verification and Validation in Computational Science and Engineering," Hermosa publishers, Albuquerque, NM.

[2] Celik, I.B., Ghia, U., Roache, P.J., Freitas, C.J., Coleman, H., and Raad, P.E., 2008, "Procedure for Estimation and Reporting of Uncertainty Due to Discretization in CFD Applications," ASME J. Fluids Eng., **130**, 078001.

[3] Cosner, R.R., Oberkampf, W.L., Rumsey, C.L., Rahaim, C.P., and Shih, T. I-P, 2006, "AIAA Committee on Standards for CFD: Status and Plans," AIAA-2006-889, 44th Aerospace Sciences Meeting, Reno, Nevada, 9-12 January.

[4] Stern, F., Wilson, R.V., Coleman, H., and Paterson, E., 2001, "Comprehensive Approach to Verification and Validation of CFD Simulations-Part 1: Methodology and Procedures," ASME J. Fluids Eng., **123**, pp. 793-802.

[5] Wilson, R. Shao, J., and Stern, F., 2004, "Discussion: "Criticisms of the "Correction Factor" Verification Method" (Roache, P., 2003, ASME J. Fluids Eng., **125**, pp. 732-733)," ASME J. Fluids Eng., **126**, pp. 704-706.

[6] Stern, F., Wilson R.V., Coleman, H.W., and Paterson, E.G., "Verification and Validation of CFD Simulations," IIHR Report No. 407, September 1999, 54pp.

[7] Eca, L., and Hoekstra, M., 2000, "An Evaluation of Verification Procedures for Computational Fluids Dynamics," 1st Report D72-7, Instituto Superior Tecnico Lisbon, Portugal.

[8] Logan, R.W. and Nitta, C.K., 2006, "Comparing 10 Methods for Solution Verification, and Linking to Model Validation," Journal of Aerospace Computing, Information, and communication, **3**, pp. 354-373.

[9] Celik, I. and Hu, G.S., 2004, "Single Grid Error Estimation Using Error Transport Equation," ASME J. Fluids Eng., **126**, pp. 778-790.

[10] ASME Performance Test Codes Committee PTC 61, 2008, "V&V 20: Standard for Verification and Validation in Computational Fluid Dynamics and Heat Transfer."

[11] Cadafalch, J., Perez-Segarra, C.D., Consul, R., and Oliva, A., 2002, "Verification of Finite Volume Computations on Steady-State Fluid Flow and Heat Transfer," ASME J. Fluids Eng., **124**, pp. 11-21.

[12] Eca, L., and Hoekstra, M., 2006, "Discretization Uncertainty Estimation Based on a Least Squares Version of the Grid Convergence Index," Proceedings of the 2nd Workshop on CFD Uncertainty Analysis, Instituto Superior Tecnico, Lisbon, October 2006.

[13] Rumsey, C.L., and Thomas, J.L., 2008, "Application of FUN3D and CFL3D to the Third Workshop on CFD Uncertainty Analysis," NASA/TM-2008-215537.

[14] Eca, L. and Hoekstra, M., Eds., 2004, "Proceedings of the Workshop on CFD Uncertainty Analysis," Lisbon, October.

[15] Xing, T. and Stern, F., 2008, "Factors of Safety for Richardson Extrapolation for Industrial Applications," IIHR report No. 466, September, 11pp.

[16] Roache, P., 2003, "Criticisms of the 'Correction Factor' Verification Method," J. Fluids Engineering, **125**, pp. 732-733.

[17] Wilson, R. and Stern, F., 2002, "Verification and Validation for RANS Simulation of a Naval Surface Combatant," Standards for CFD in the Aerospace Industry, AIAA paper 2002-0904 Aerospace Sciences Meeting, Reno, Nevada.

[18] Kreyszig, E., "Advanced Engineering Mathematics," 7th edition, John Wiley & Sons, Inc., 1993, pp. 1148-1271.

[19] Ross, S.M., 2003, "Peirce's Criterion for the Elimination of Suspect Experimental Data," J. of Eng. Tech.

[20] Bruneau, C.H. and Saad, M., 2006, "The 2D Lid-driven Cavity Problem Revisited," Computers & Fluids, **35**, pp. 326-348.

[21] Botella, O. and Peyret, R., 1998, "Benchmark Spectral Results on the Lid-driven Cavity Flow," Computers & Fluids, **27**(4), pp. 421-433.

[22] Hortmann, M., Peric, M., and Scheuerer, G., 1990, "Multigrid Benchmark Solutions for Laminar Natural Convection Flows in Square Cavities," ASME FED, **93**, pp. 1-6.

[23] Celik, I., and Karatekin, O., 1997, "Numerical Experiments on Application of Richardson Extrapolation with Nonuniform Grids," ASME J. Fluids Eng., **119**, pp. 584-590.

[24] Thangam, S. and Speziale, C.G., 1992, "Turbulent Flow Past a Backward-Facing Step: A Critical Evaluation of Two-Equation Models," AIAA J., **30** (5), pp. 1314-1320.

[25] Avva, R.K., Kline, S.J., and Ferziger, J.H., 1998, "Computation of Turbulent Flow over a Backward-Facing Step-Zonal Approach," AIAA 26th Aerospace Sciences Meeting, January 11-14, 1988/Reno, Nevada.

[26] Pérez-Segarra, C.D., Oliva, A., and Consul, R., 1996, "Analysis of some Numerical Aspects in the Solution of the Navier-Stokes Equations using Non-Orthogonal Collocated Finite-Volume Methods," Proceedings of the Third ECCOMAS Computational Fluid Dynamics Conference, pp. 505-511, Wiley, Paris, France.

[27] Demirdzic, I., Lilek, Z., and Peric, M., 1992, "Fluid Flow and Heat Transfer Test Problems for Non-Orthogonal Grids: Bench-Mark Solutions," Int. J. Numer. Methods Fluids, **15**, pp. 329-254.

[28] Pérez-Segarra, C.D., Oliva, A., Costa, M., and Escanes, F., 1995, "Numerical Experiments in Turbulent Natural and Mixed Convection in Internal Flows," Int. J. Numer. Methods Heat Fluid Flow, **5**, pp. 13-33.

[29] Pérez-Segarra, C.D., Cadafalch, J., Rigola, J., and Oliva, A., 1999, "Numerical Study of Turbulent Fluid Flow through Valves," Proceedings of the International Conference on Compressors and Their Systems, City University, London, pp. 13-14.

[30] Sommers, L.M.T., 1994, PhD thesis, Technical University of Eindhoven.

[31] Soria, M., Cadafalch, J., Cònsul, R., and Oliva, A., 2000, "A Parallel Algorithm for the Detailed Numerical Simulation of Reactive Flows," Proceedings of the 1999 Parallel Computational Fluid Dynamics Conference, pp. 389-396, Williamsburg, VA.

[32] Xing, T., Carrica, P., Stern, F., 2008, "Computational Towing Tank Procedures for Single Run Curves of Resistance and Propulsion," ASME J. Fluids Eng., **130**, 101102, pp. 1-14

[33] Carrica, P.M., Wilson, R.V., and Stern, F., 2007, "An Unsteady Single-phase Level Set Method for Viscous Free Surface Flows," Int. J. Numer. Meth. Fluids, **53** (2), pp. 229-256.

Appendix 1. Analytical and Numerical Benchmarks

Study 1 One-Dimensional Wave Equation

As shown in Figure A1, with the refinements of the grids, the errors monotonically decrease and solutions approach the AR as CF changes from CF = 0.4 on the coarsest grid to CF = 1 on the finest grid. FS_A for GCI and GCI_C are the same as CF < 1 and smaller than that predicted by the FS method except at CF = 1 where FS_A using the three methods are the same. FS_A for GCI and GCI_C are smaller and larger than those predicted by the CF method for CF < 0.875 and 0.875 < CF < 1, respectively. FS_A of the FS method are smaller and larger than those predicted by the CF method for CF < 0.8 and 0.8 < CF < 1, respectively. These observations are consistent with the FS shown in Figure 1. The average FS_A are 1.44, 1.44, 1.61, and 1.60 for GCI, GCI_C, CF, and FS methods, respectively. The standard deviations of FS_A are 0.27, 0.27, 0.78, and 0.49 for GCI, GCI_C, CF, and FS methods, respectively.

Study 2 Two-Dimensional Laplace Equation

As shown in Figure A2, with the refinements of the grids, the errors monotonically decrease. Solutions approach the AR (CF = 1) monotonically for constant Dirichlet boundary conditions and oscillatorily for non-constant value Dirichlet boundary conditions. Comparison of FS_A magnitudes for different methods shows similar trend as discussed in study 1 and shown in Figure 1. The average FS_A are 1.30, 1.31, 1.23, and 1.38 for GCI, GCI_C, CF, and FS methods, respectively. The standard deviations of FS_A are 0.04, 0.04, 0.09, and 0.07 for GCI, GCI_C, CF, and FS methods, respectively.

Study 3 Two-Dimensional Driven Cavity (Re=1,000)

As shown in Figure A3, only two sets of grid study are available and thus it is difficult to draw any conclusions on the convergence characteristics when the grids are refined.

However, CF is closer to 1 and errors decrease with the refinements of the grids. One exception is for the minimum stream function using the BS scheme, which shows a larger Ug on the finer grid. Comparison of FS_A magnitudes for different methods shows similar trend as shown in Figure 1. All verification methods except the FS method predict $FS_A < 1$ for CF > 1. The average FS_A are 1.12, 1.16, 1.23, and 1.58 for GCI, GCI_C, CF, and FS methods, respectively. The standard deviations of FS_A are 0.41, 0.37, 0.51, and 0.62 for GCI, GCI_C, CF, and FS methods, respectively.

Study 4 Two-Dimensional Natural Convection Flows in Square Cavities (Ra=10^4)

As shown in Figure A4, all variables have 3 grid-triplet studies except U_{mon} that has only two grid-triplet study. When grids are refined, all errors monotonically decrease and all variable solutions either linearly or oscillatorily approach the AR (CF = 1). Comparison of FS_A magnitudes for different methods shows similar trend as shown in Figure 1. FS_A oscillatorily decrease when CF is approaching the AR from CF < 1. For CF > 1, GCI_C predicted higher FS_A than GCI and CF methods. For CF > 1.16, uncertainty estimates using GCI do not bound the true error ($FS_A < 1$) and GCI_C and CF have similar magnitudes of FS_A around 1.4 while the FS method has much larger FS_A. The average FS_A are 1.49, 1.55, 1.75, and 1.90 for GCI, GCI_C, CF, and FS methods, respectively. The standard deviations of FS_A are 0.26, 0.25, 0.68, and 0.45 for GCI, GCI_C, CF, and FS methods, respectively.

Study 5 Two-Dimensional Natural Convection Flows in Square Cavities (Ra=10^5)

As shown in Figure A5, all variables have 4 grid-triplet studies. When the grids are refined, all errors monotonically decrease except the two coarsest sets of grids for U_{max} and all variable solutions either monotonically or oscillatorily approach the AR. Similar to the previous studies, uncertainty estimates using GCI, GCI_C, and CF methods do not bound the true error for some points at CF > 1 ($FS_A < 1$) while the FS method always bounds the true error ($FS_A < 1$). The average FS_A are 1.84, 1.96, 2.64, and 2.74 for GCI,

GCI$_C$, CF, and FS methods, respectively. The standard deviations of FS$_A$ are 0.74, 0.73, 1.77, and 1.48 for GCI, GCI$_C$, CF, and FS methods, respectively.

Study 6 Two-Dimensional Natural Convection Flows in Square Cavities (Ra=10^6)

As shown in Figure A6, the number of grid-triplet studies is 5 for all variables except 4 for U$_{max}$ and Nu$_{max}$ and 2 for V$_{max}$. When the grids are refined, all errors monotonically decrease and all variable solutions either monotonically or oscillatorially approach the AR. Similar to the previous studies, GCI, GCI$_C$, and CF methods do not bound the true error for some points at CF > 1 while the FS method always bounds the true error. The average FS$_A$ are 1.47, 1.53, 1.91, and 1.89 for GCI, GCI$_C$, CF, and FS methods, respectively. The standard deviations of FS$_A$ are 0.40, 0.40, 0.99, and 0.64 for GCI, GCI$_C$, CF, and FS methods, respectively.

Study 7 Two-Dimensional Backward-Facing Step

As shown in Figure A7, with the refinement of the grids, the errors oscillatorially decrease with several orders of magnitude larger than those in other studies and solutions approach the AR with huge oscillations of CF. This suggests that the grids are still far from the AR for such a high Reynolds number flows. When CF > 1.4, GCI does not bound the true error while all other methods bounded the true error with FS$_A$ predicted by the FS method is the largest. The average FS$_A$ are 0.92, 1.39, 1.49, and 15.08 for GCI, GCI$_C$, CF, and FS methods, respectively. The standard deviations of FS$_A$ are 0.33, 0.15, 0.22, and 19.12 for GCI, GCI$_C$, CF, and FS methods, respectively.

Study 8 Square Cavity with Moving Top Wall (Re=100)

As shown in Figure A8, 4 variables only have two grid-triplet studies and 3 variables have 3 grid-triplet studies, which suggests that further refinement of the grids are necessary. However, all variable errors linearly decrease when the grids are refined. When CF ≥ 1.4, all methods except GCI predict enough uncertainty estimates to bound

the true errors. The average FS_A are 1.56, 1.96, 2.20, and 6.27 for GCI, GCI_C, CF, and FS methods, respectively. The standard deviations of FS_A are 0.48, 0.45, 0.78, and 6.38 for GCI, GCI_C, CF, and FS methods, respectively.

Study 9 Square Cavity with Moving Top Wall (Re=1,000)

As shown in Figure A9, all variables only show monotonic convergence on two grid-triplet studies except 3 grid studies for the x velocity using UDS at 0 degree. When the grids are refined, errors for UDS-x velocity-0 degree oscillatorially decrease while errors for all other variables linearly decrease. When CF = 1 and 1.15, all methods fail to bound the true error except the FS method. The average FS_A are 2.42, 2.46, 4.12, and 3.32 for GCI, GCI_C, CF, and FS methods, respectively. The standard deviations of FS_A are 1.55, 1.52, 3.72, and 2.41 for GCI, GCI_C, CF, and FS methods, respectively.

Study 10 Cubic Cavity with Moving Top Wall (Re=100)

As shown in Figure A10, only two grid-triplet studies are available. However, all errors linearly decrease when the grids are refined. Uncertainty estimates predicted by all methods bound the true errors. The average FS_A are 2.76, 2.90, 3.93, and 4.10 for GCI, GCI_C, CF, and FS methods, respectively. The standard deviations of FS_A are 1.43, 1.28, 2.72, and 1.61 for GCI, GCI_C, CF, and FS methods, respectively.

Study 11 Axisymmetric Turbulent Flow through a Valve

As shown in Figure A11, similar to study 10, only two grid-triplet studies are available and thus no conclusive behavior of the variables to approach the AR can be drawn. However, all errors linearly decrease when the grids are refined. Uncertainty estimates predicted by all methods bound the true errors. The average FS_A are 3.22, 3.22, 5.89, and 4.46 for GCI, GCI_C, CF, and FS methods, respectively. The standard deviations of FS_A are 2.58, 2.58, 5.14, and 3.73 for GCI, GCI_C, CF, and FS methods, respectively.

Study 12 One-Dimensional Steady-State Convection-Diffusion Process without Source Term

As shown in Figure A12, all variables have four grid-triplet studies. When the grids are refined, errors for all variables decrease and solutions are approaching the AR. Uncertainty estimates of all methods bound the true errors except at CF = 0.91 where only the FS method bound the true error. The average FS_A are 1.50, 1.51, 1.51, and 1.63 for GCI, GCI_C, CF, and FS methods, respectively. The standard deviations of FS_A are 0.35, 0.34, 0.41, and 0.38 for GCI, GCI_C, CF, and FS methods, respectively.

Study 13 Heat Transfer from Isothermal Cylinder Enclosed by a Square Duct

As shown in Figure A13, only two grid-triplet studies are available for all the variables except 3 grid-triplet studies for the UDS-temperature. When the grids are refined, all errors linearly decrease except the uncertainty estimates using GCI, GCI_C, and CF methods for temperature with the SMART scheme increase. When $1.2 < CF < 1.4$, uncertainty estimates predicted by all the methods do not bound the true errors except the FS method. The average FS_A are 1.39, 1.63, 1.65, and 2.50 for GCI, GCI_C, CF, and FS methods, respectively. The standard deviations of FS_A are 0.47, 0.47, 0.33, and 0.81 for GCI, GCI_C, CF, and FS methods, respectively.

Study 14 Premixed Methane/Air Laminar Flat Flame on a Perforated Burner

As shown in Figure A14, there are 5 and 4 grid-triplet studies for UDS and SMART methods, respectively. When the grids are refined, errors for most variables continuously decrease, solutions using the UDS method approach the AR either linearly or oscillatorily, and solutions using the SMART method show oscillations far away from the AR. For CF close to 1, GCI, GCI_C and CF predict FS_A around 1. For CF > 1, FS_A predicted by the three methods show large oscillations of which some values are below 1. The FS method always provides sufficient large FS_A. However, there is one grid-triplet study at CF = 0.51 where none of the methods can bound it. The reason behind this is

unknown. The average FS_A are 1.63, 1.66, 2.13, and 2.25 for GCI, GCI_C, CF, and FS methods, respectively. The standard deviations of FS_A are 0.35, 0.35, 0.87, and 1.02 for GCI, GCI_C, CF, and FS methods, respectively.

Study 15 Data for "Exact" Grid Convergence Set

As shown in Figure A15, solutions for the "exact" grid convergence study are always in the AR when there is no perturbation or with perturbation #4. Other cases only have two grid-triplet studies. Overall errors decrease when the grids are refined. For CF > 1 when solutions are far away from the AR, FS_A for the FS method increases while FS_A for other methods decrease. The average FS_A are 1.79, 1.81, 2.24, and 2.18 for GCI, GCI_C, CF, and FS methods, respectively. The standard deviations of FS_A are 0.85, 0.88, 1.76, and 1.44 for GCI, GCI_C, CF, and FS methods, respectively.

Study 16 Beam Bending Problem for 2nd Series on Grid Convergence

As shown in Figure A16, there are 3 grid-triplet studies for the three codes investigated. When the grids are refined, both the errors and the correction factors show oscillations. Uncertainty estimates predicted by all methods fail to bound the true errors when 0.6 < CF < 1.2. The average FS_A are 0.59, 0.64, 1.00, and 0.96 for GCI, GCI_C, CF, and FS methods, respectively. The standard deviations of FS_A are 0.068, 0.061, 0.228, and 0.095 for GCI, GCI_C, CF, and FS methods, respectively.

Study 17 Beam Bending Problem for 3rd Series on Grid Convergence

As shown in Figure A17, there are only two grid-triplet studies for the three codes investigated. When the grids are refined, the errors decrease. Uncertainty estimates predicted by all methods fail to bound the true errors when CF > 1.3. The average FS_A are 0.97, 1.03, 1.69, and 1.52 for GCI, GCI_C, CF, and FS methods, respectively. The standard deviations of FS_A are 0.58, 0.52, 1.31, and 0.68 for GCI, GCI_C, CF, and FS methods, respectively.
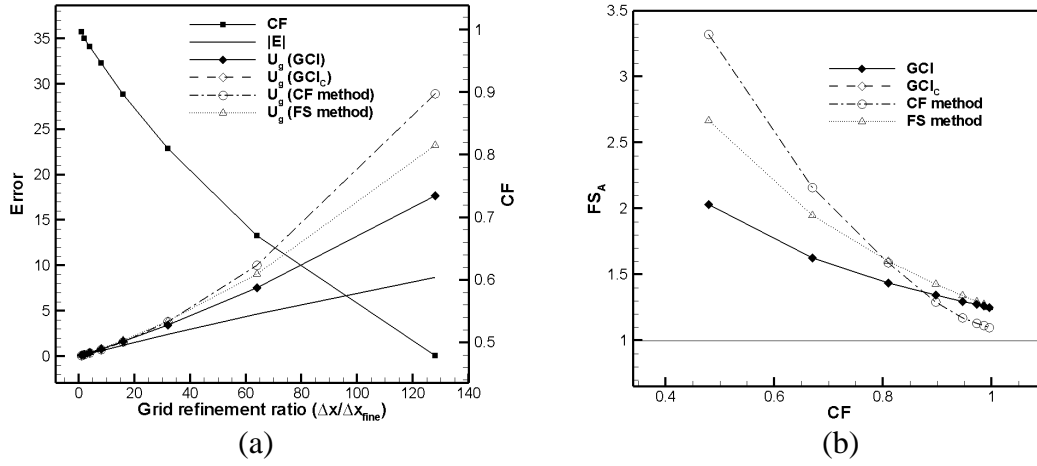
Figure A1: 1D Wave Equation [6]: (a) error, uncertainties, and correction factor, (b) actual factor of safety
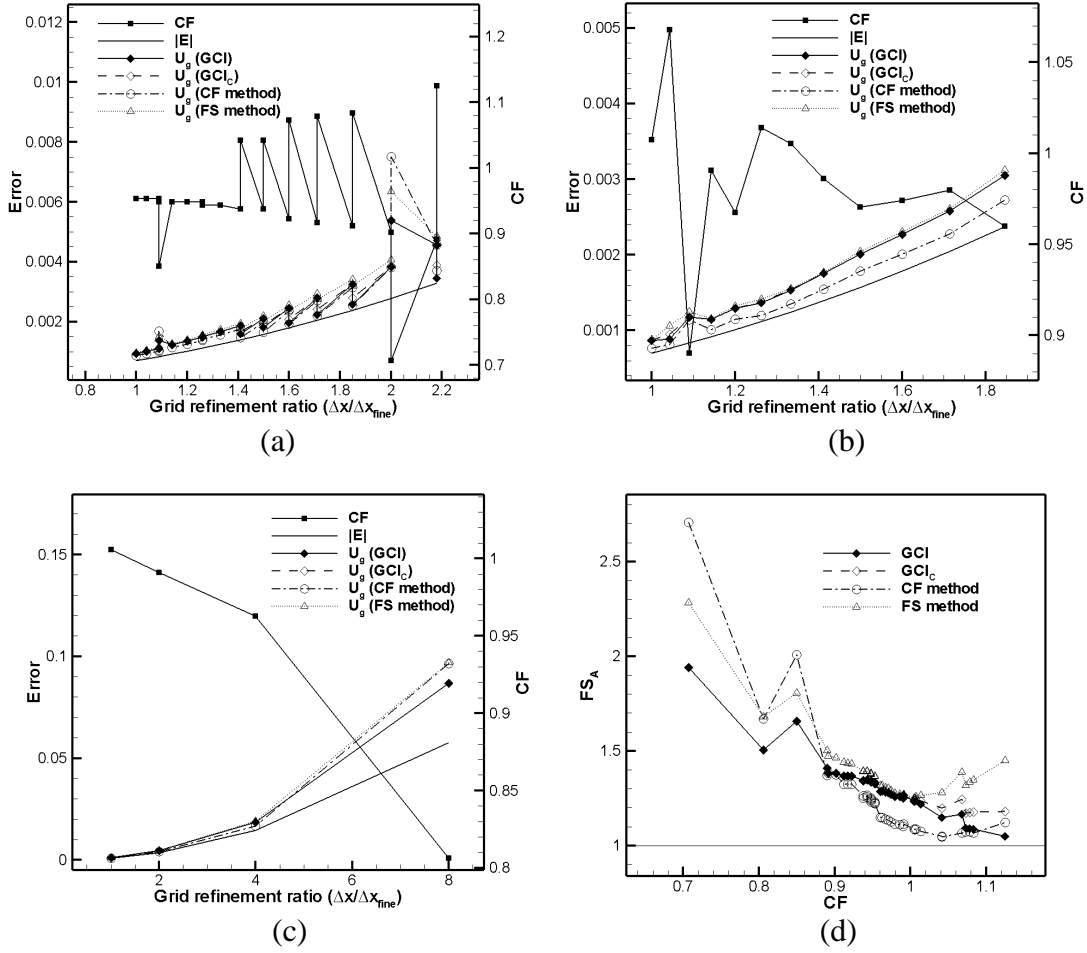
Figure A2: 2D Laplace Equation [5,7]: (a) non-constant value Dirichlet boundary conditions (Eca and Hoekstra, 2000), (b) non-constant value Dirichlet boundary conditions (Iowa recalculated), (c) constant value Dirichlet boundary conditions (Iowa calculation), (d) actual factor of safety.

(a)

(b)

(c)

(d)

(e)

(f)

(g)   (h)
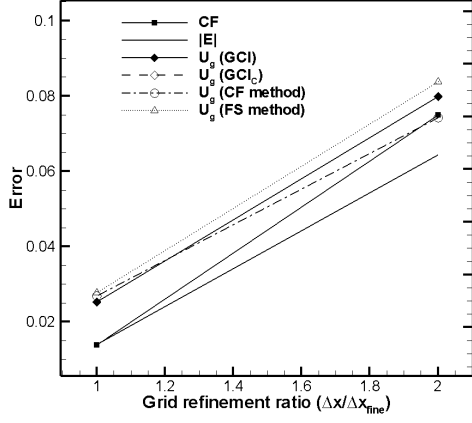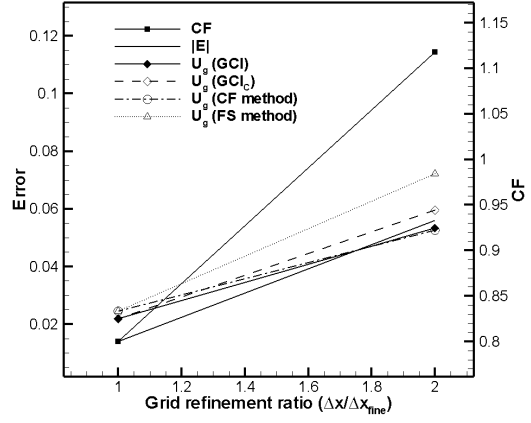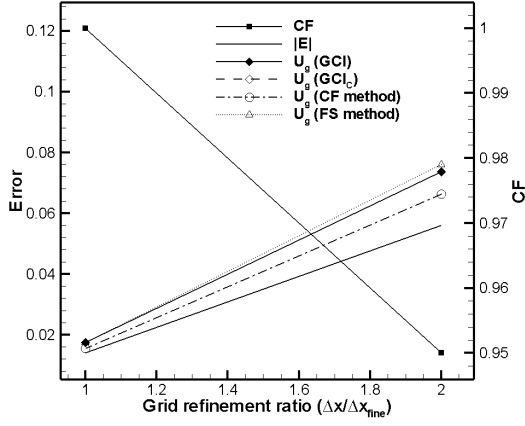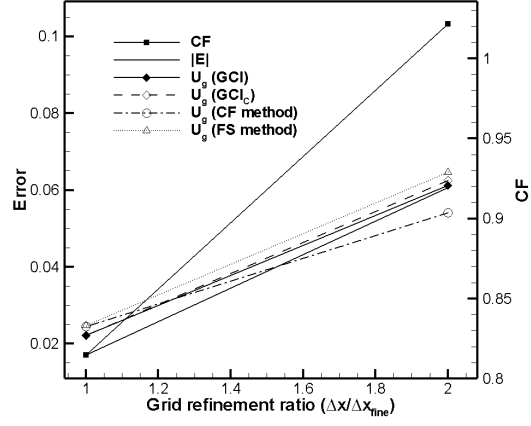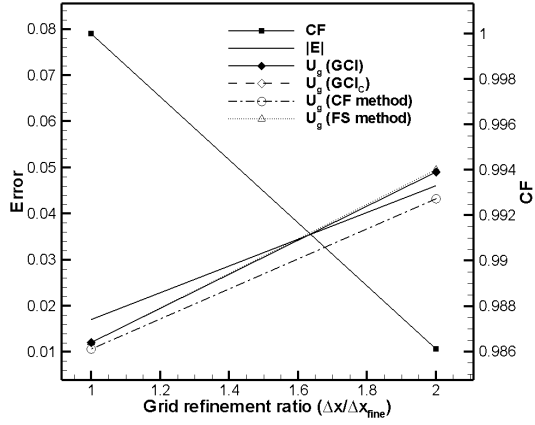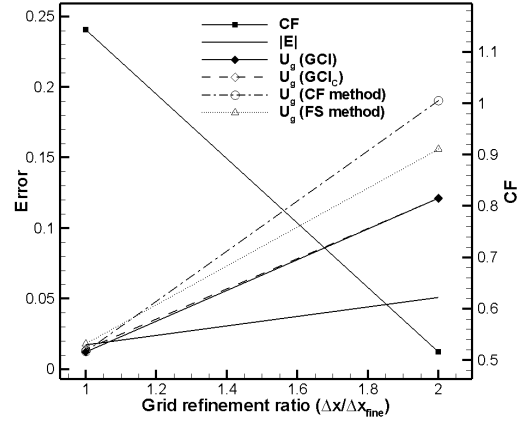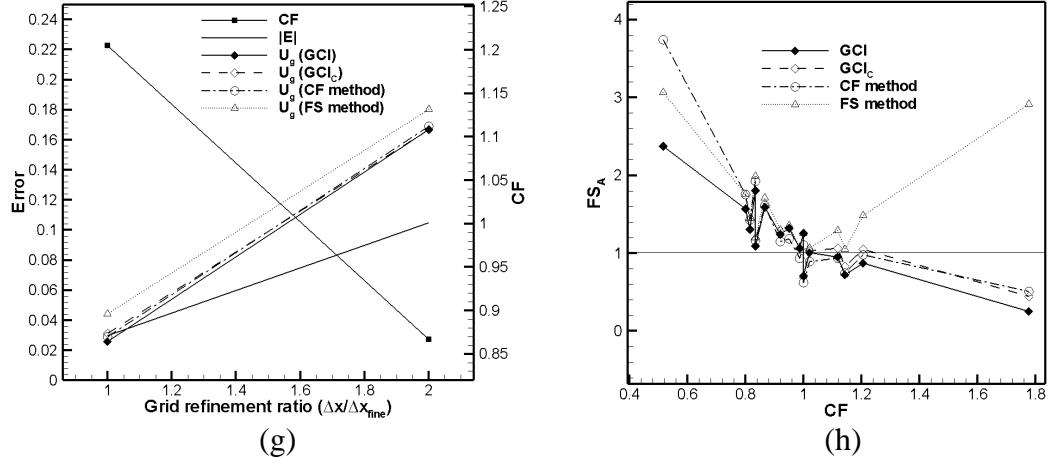
Figure A3: 2D Driven Cavity [20, 21]: (a) maximum stream function using BS scheme, (b) maximum stream function using upwind 3 scheme, (c) maximum stream function Kawamura scheme, (d) maximum vorticity using BS scheme, (e) maximum vorticity using upwind-3 scheme, (f) maximum vorticity using Kawamura scheme, (g) minimum stream function using BS scheme, (h) actual factor of safety.

(a)

(b)

(c)

(d)

(e)

(f)

(g)　　　　　　　　　　　　　　　　　　(h)
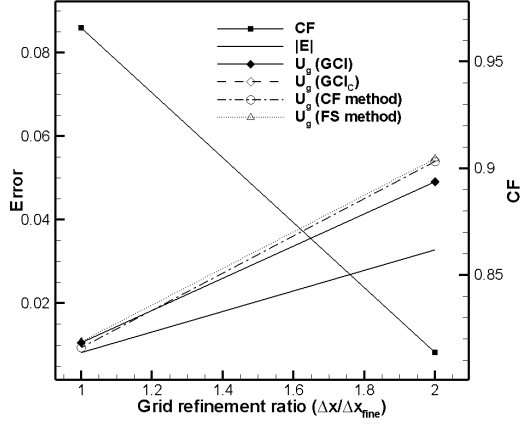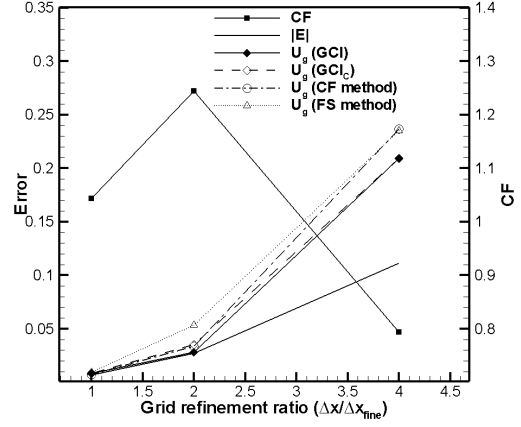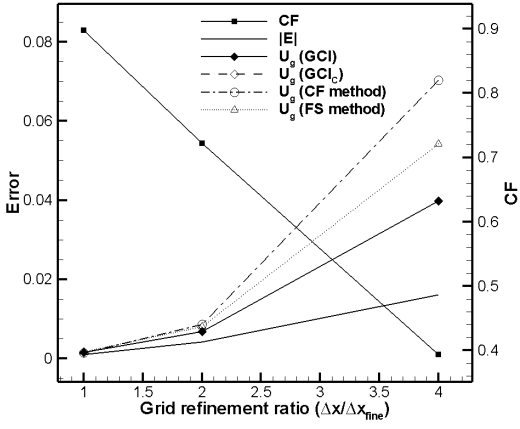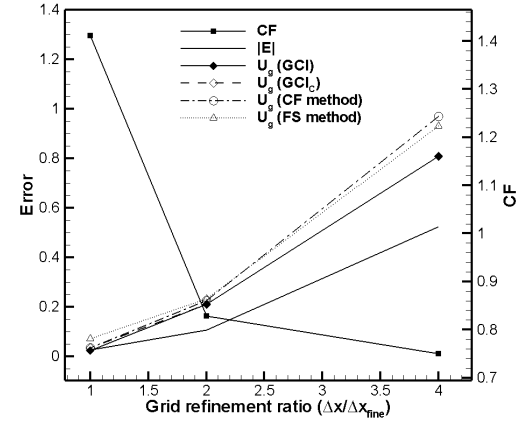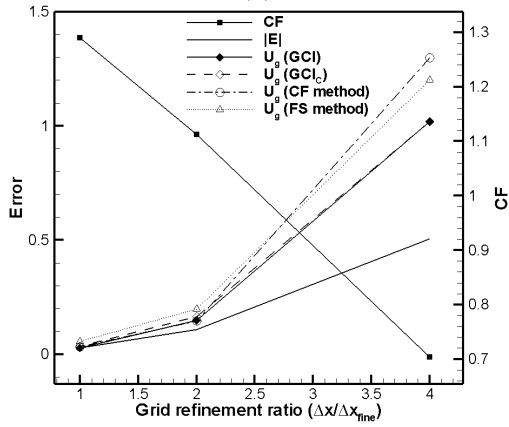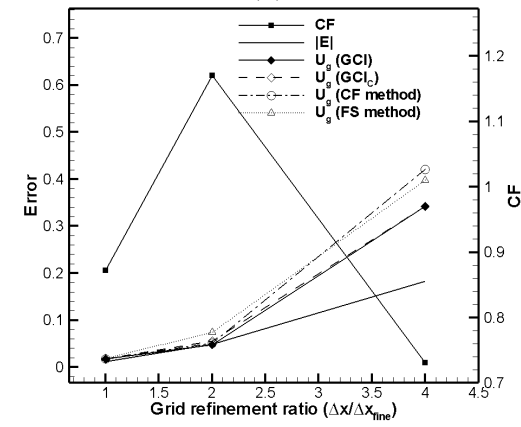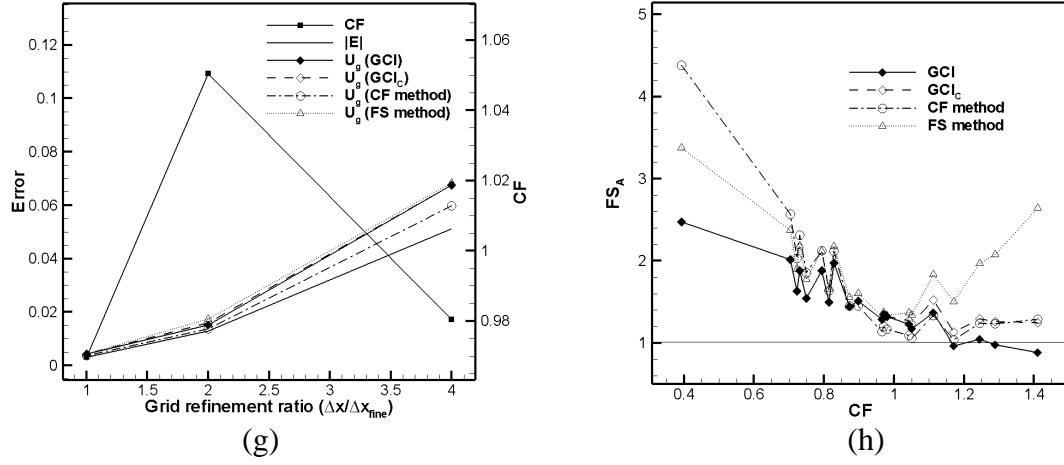
Figure A4: 2D Natural Convection Flows in Square Cavities at Ra=10^4 [22]: (a) U$_{mon}$, (b) V$_{mon}$, (c) T$_{mon}$, (d) U$_{max}$, (e) V$_{max}$, (f) Nu$_{max}$, (g) Nu, (h) actual factor of safety.
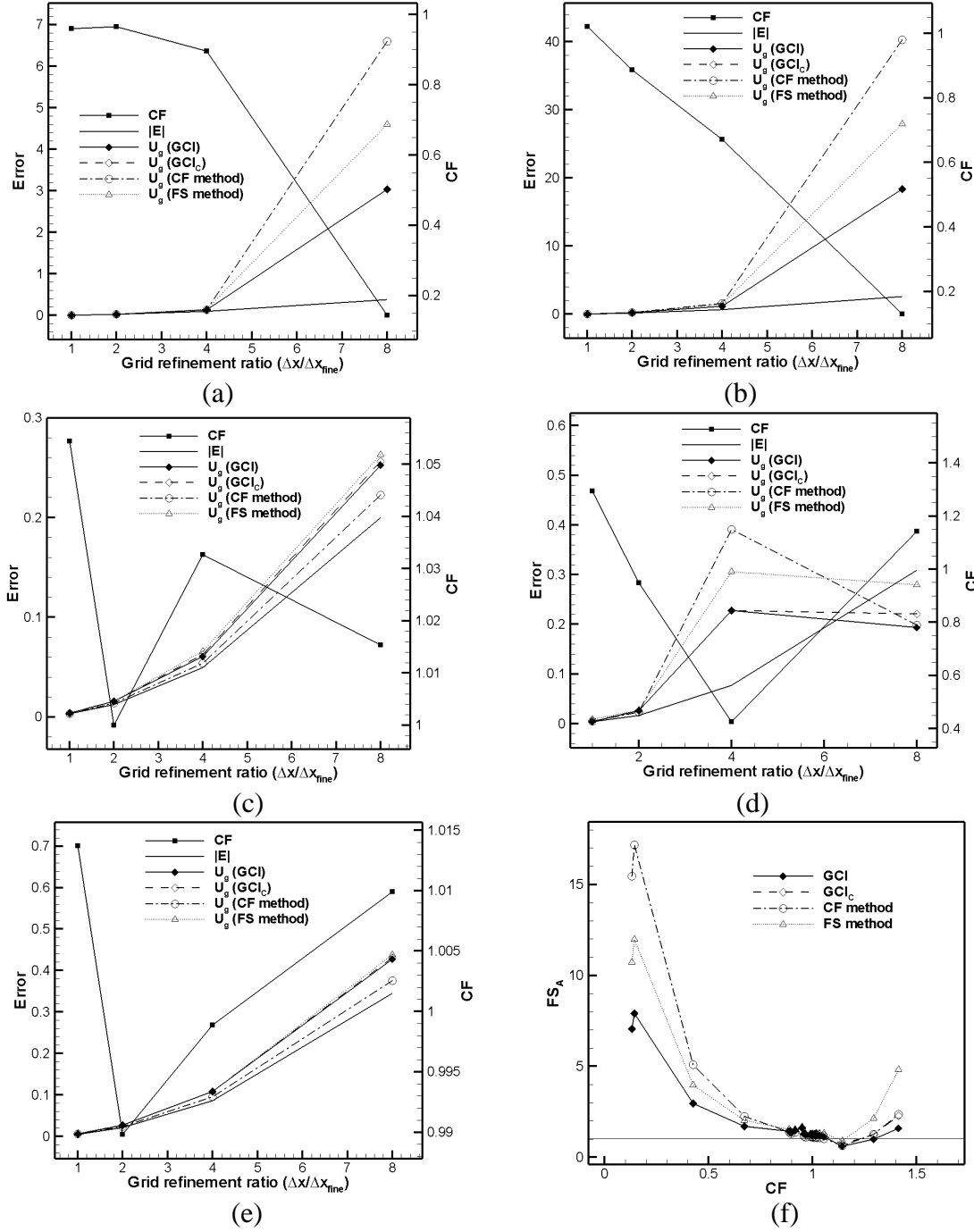
Figure A5: 2D Natural Convection Flows in Square Cavities at Ra=10^5 [22]: (a) U_{mon}, (b) V_{mon}, (c) T_{mon}, (d) U_{max}, (e) Nu, (f) actual factor of safety.
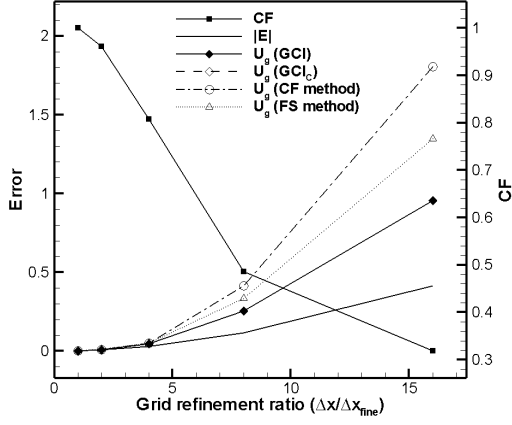
(a)
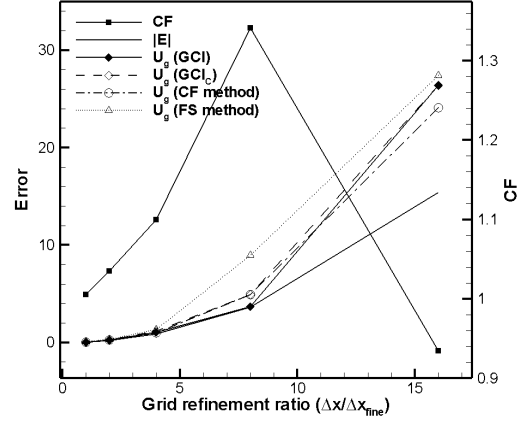
(b)
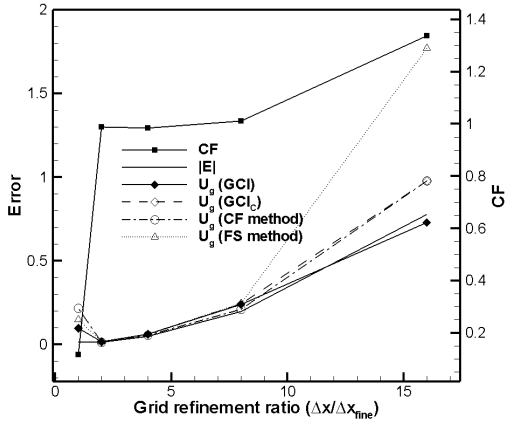
(c)
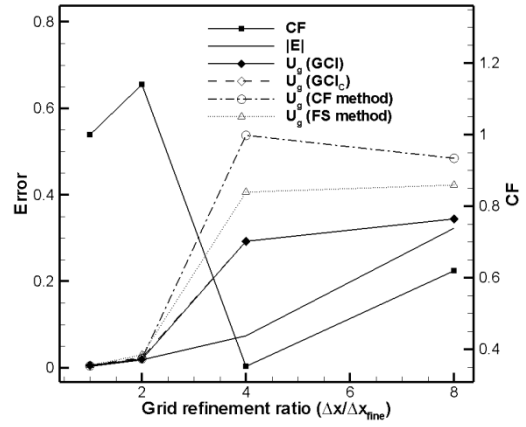
(d)
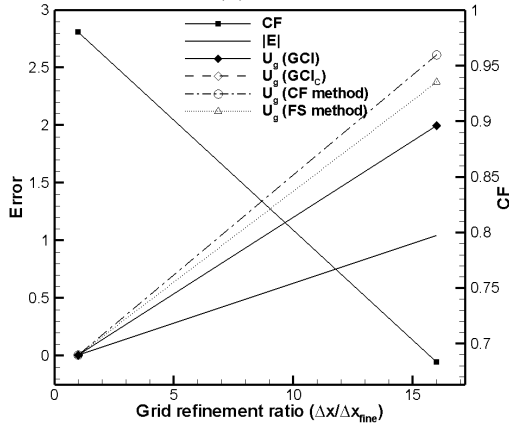
(e)
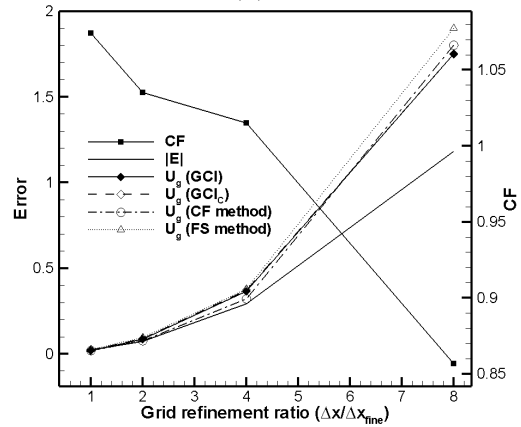
(f)
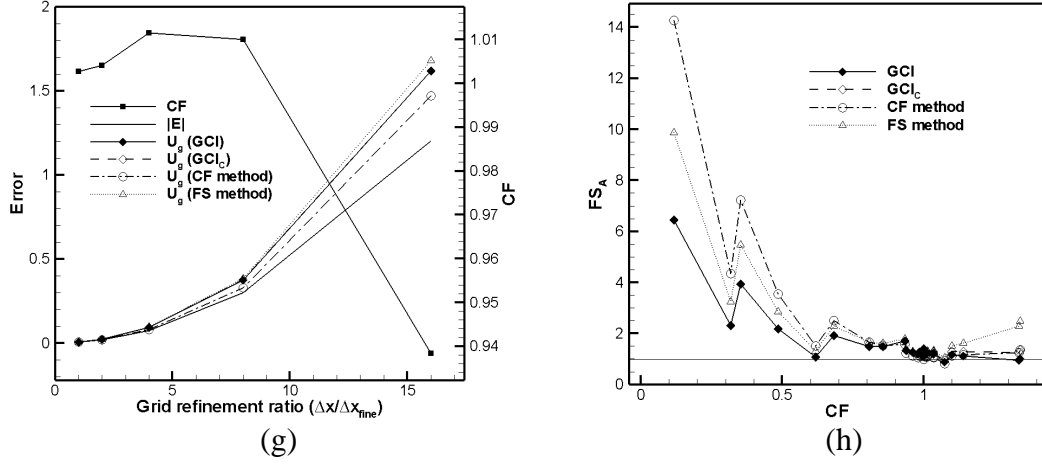
Figure A6: 2D Natural Convection Flows in Square Cavities at Ra=10^6 [22]: (a) U_{mon}, (b) V_{mon}, (c) T_{mon}, (d) U_{max}, (e) V_{max}, (f) Nu_{max}, (g) Nu, (h) actual factor of safety.
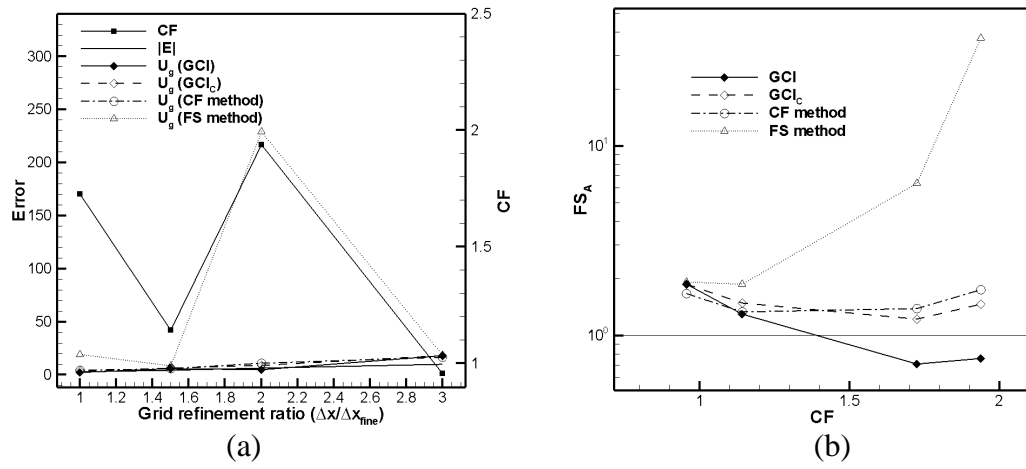
Figure A7: 2D Backward-facing Step at Re=1.5×10^5 [23, 24, 25]: (a) error, uncertainties, and correction factor, (b) actual factor of safety
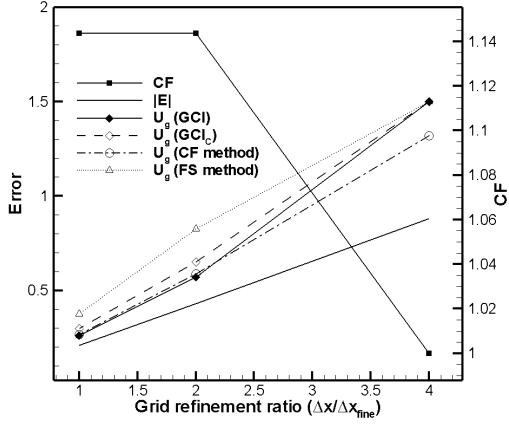
(a)
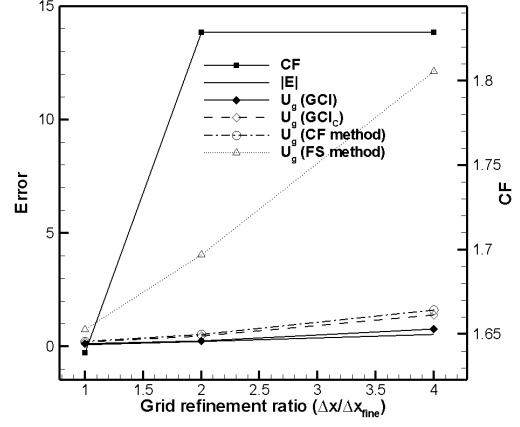
(b)
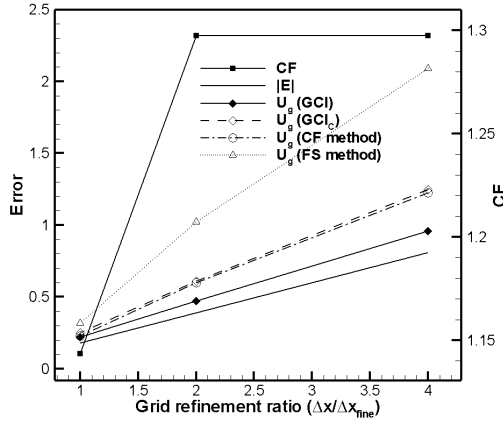
(c)
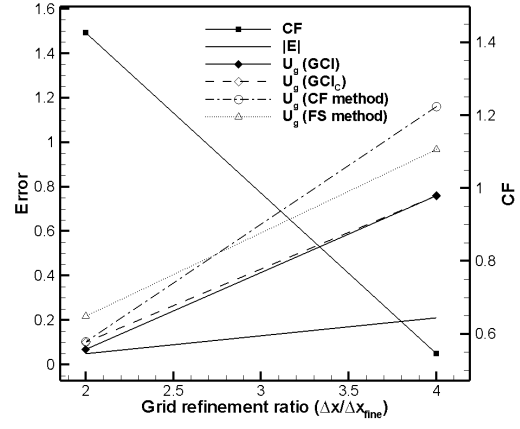
(d)
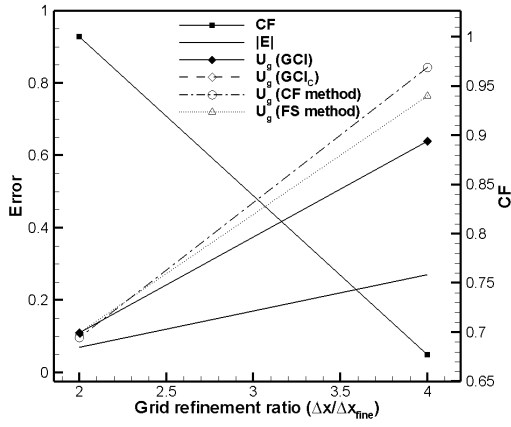
(e)
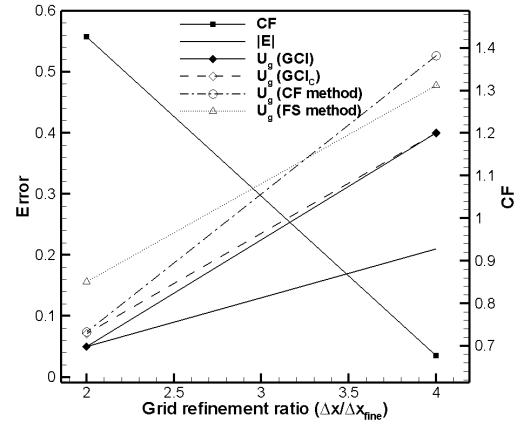
(f)
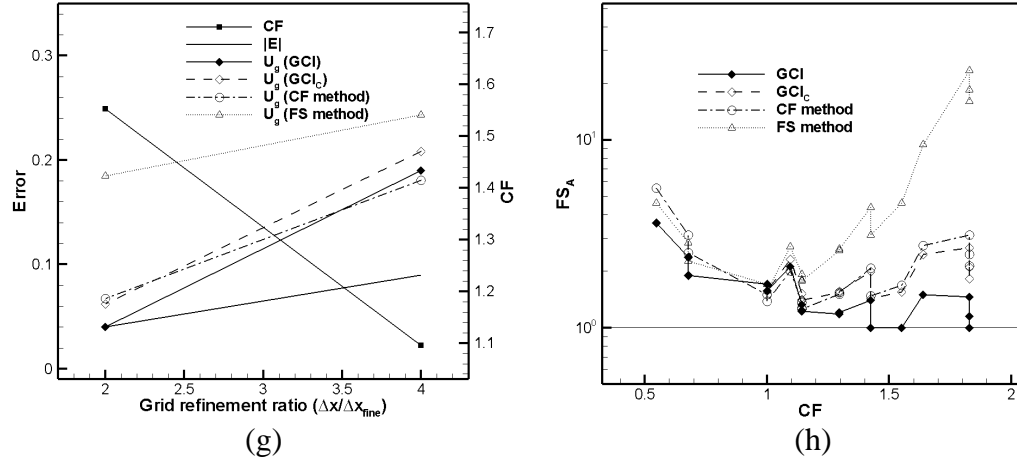
Figure A8: Square cavity with moving top wall, Re=100 [26, 27]: (a) UDS-x velocity-0 deg; (b) UDS-x velocity-60 deg; (c) UDS-y velocity-0 deg; (d) SMART-x velocity-0 deg; (e) SMART-x velocity-60 deg; (f) SMART-y velocity-0 deg; (g) SMART-y velocity-60 deg; (h) actual factor of safety.
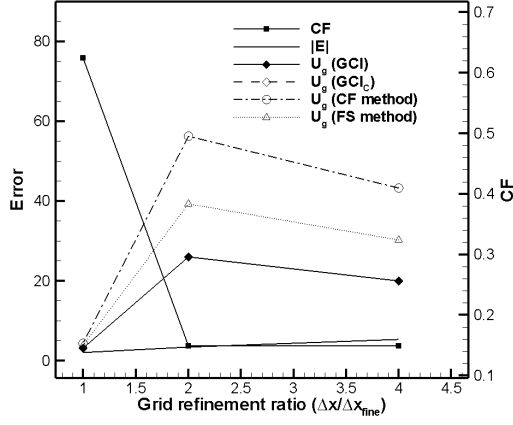
(a)
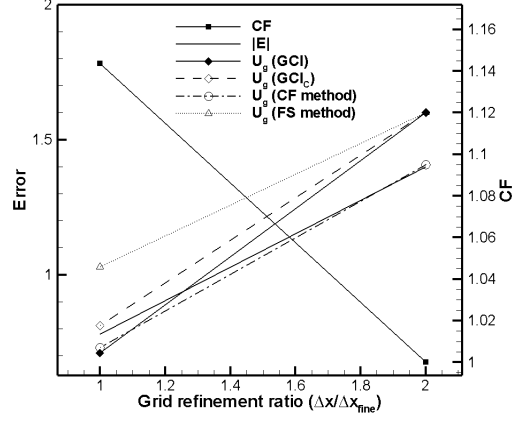
(b)
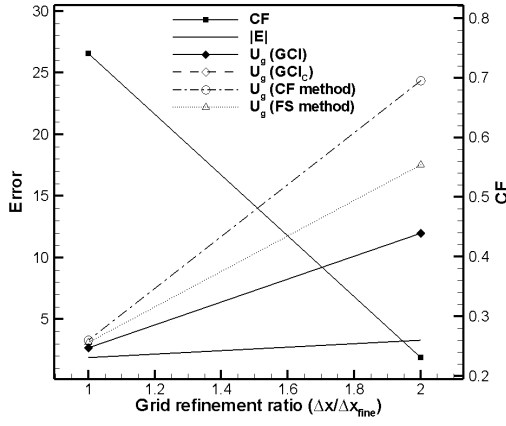
(c)
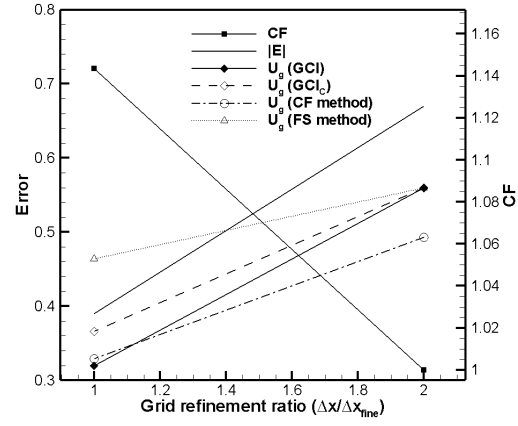
(d)
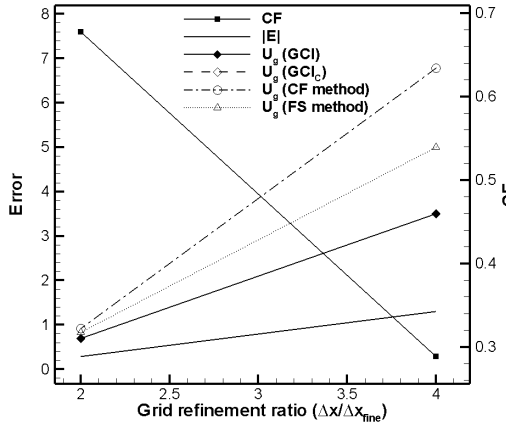
(e)
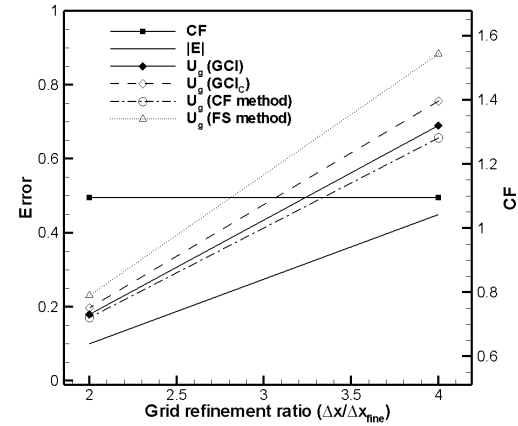
(f)
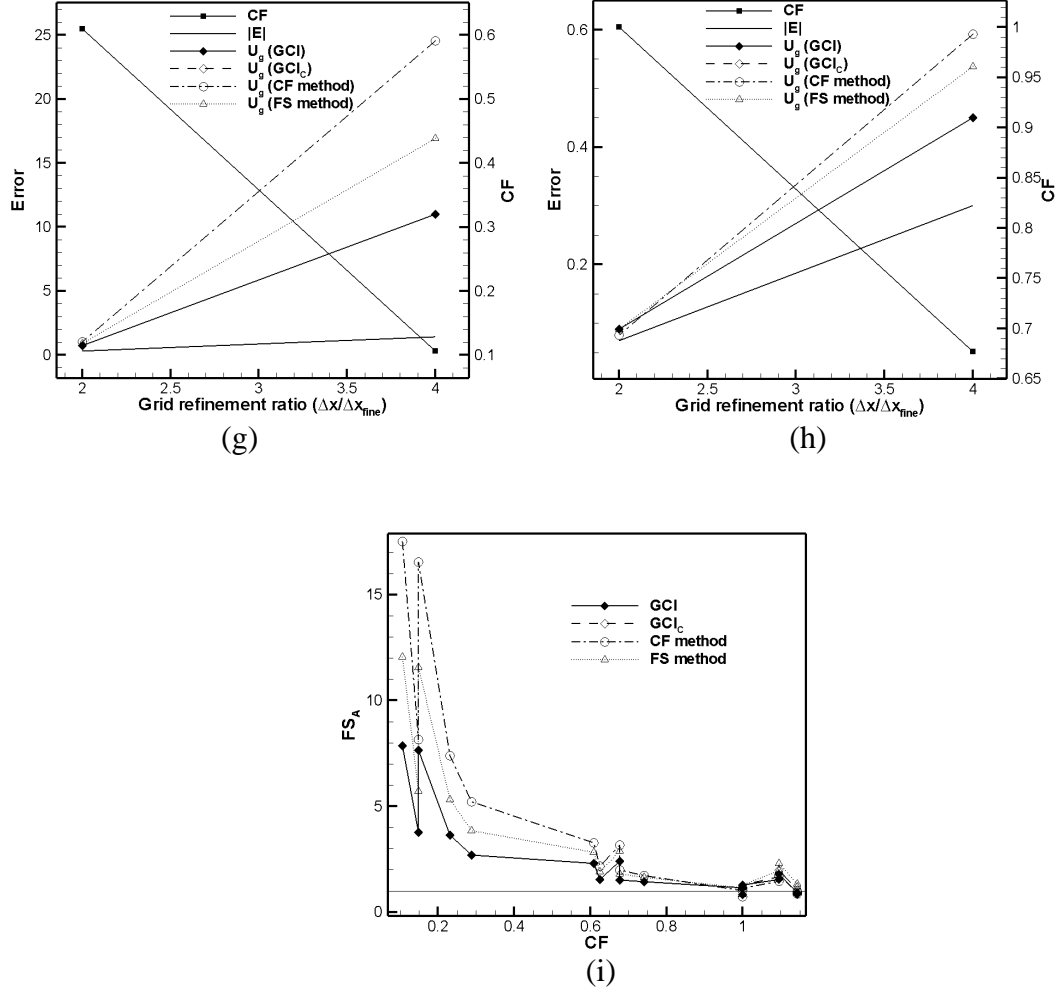
Figure A9: Square cavity with moving top wall at Re=1000 [26, 27]: (a) UDS-x velocity-0 deg; (b) UDS-x velocity-60 deg; (c) UDS-y velocity-0 deg; (d) UDS-y velocity-60 deg; (e) SMART-x velocity-0 deg; (f) SMART-x velocity-60 deg; (g) SMART-y velocity-0 deg; (h) SMART-y velocity-60 deg; (i) actual factor of safety.
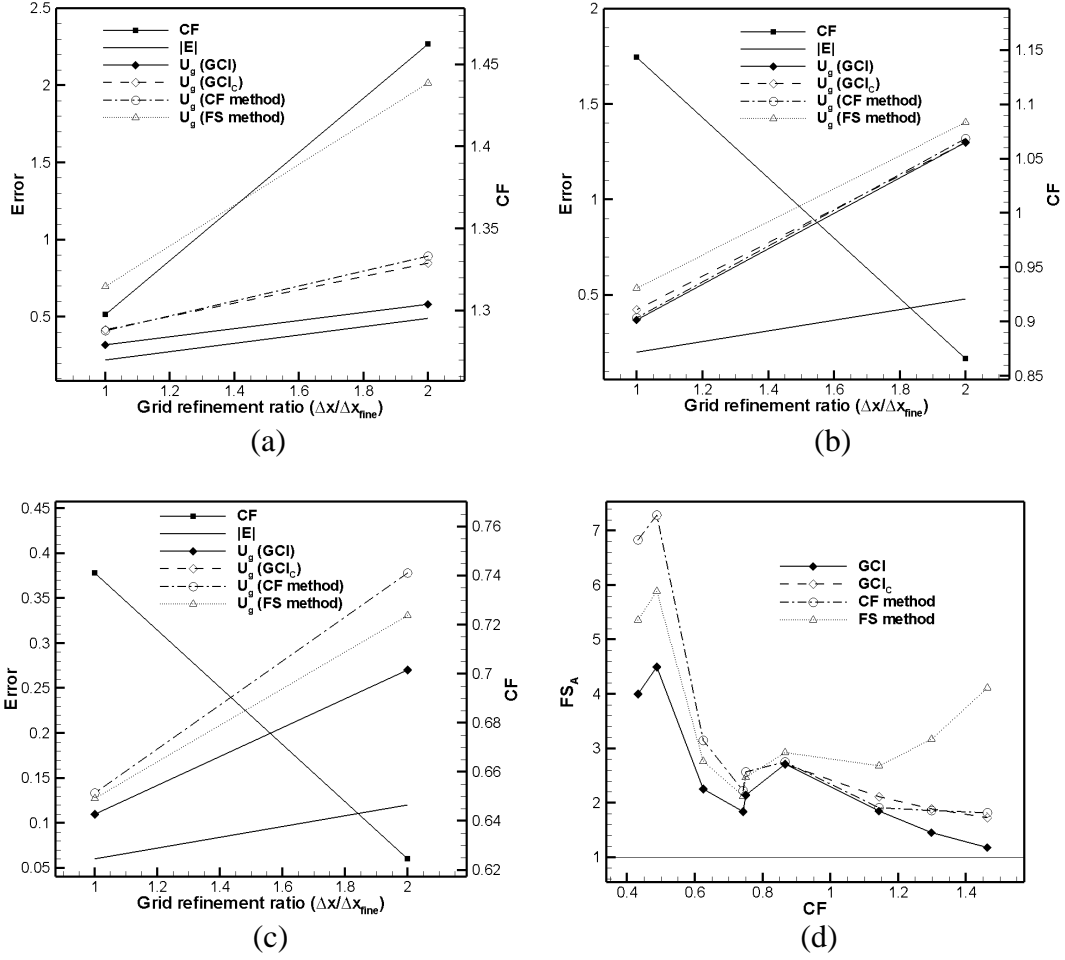
Figure A10: Cubic cavity with moving top wall, Re=100 [26, 27]: (a) x-velocity-UDS; (b) y-velocity-UDS; (c) z-velocity-UDS, (d) actual factor of safety.
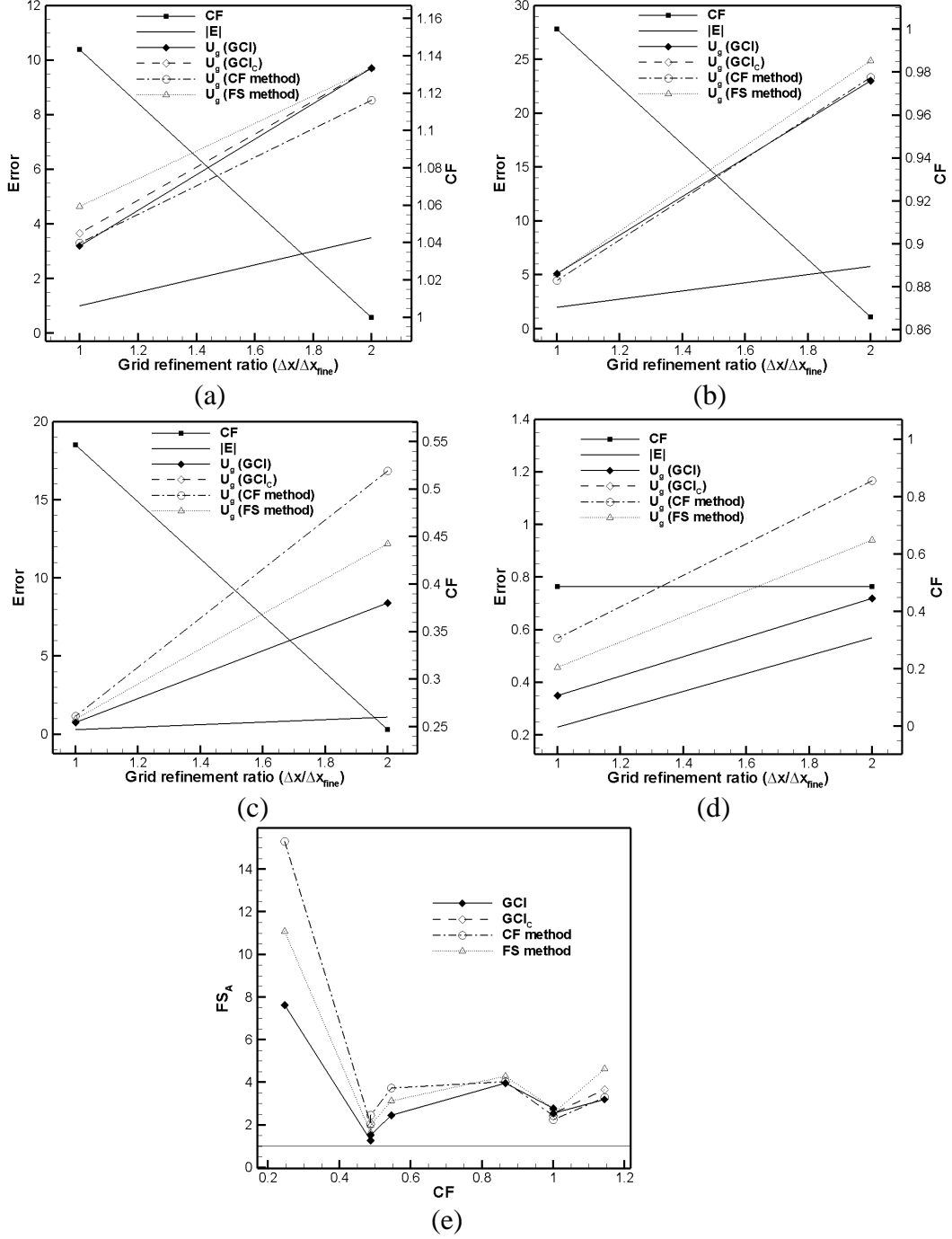
Figure A11: Axisymmetric turbulent flow through a valve [28, 29]: (a) TKE-PLDS; (b) dissipation rate of TKE-PLDS; (c) radial-velocity-SMART; (d) axial-velocity-SMART; (e) actual factor of safety.
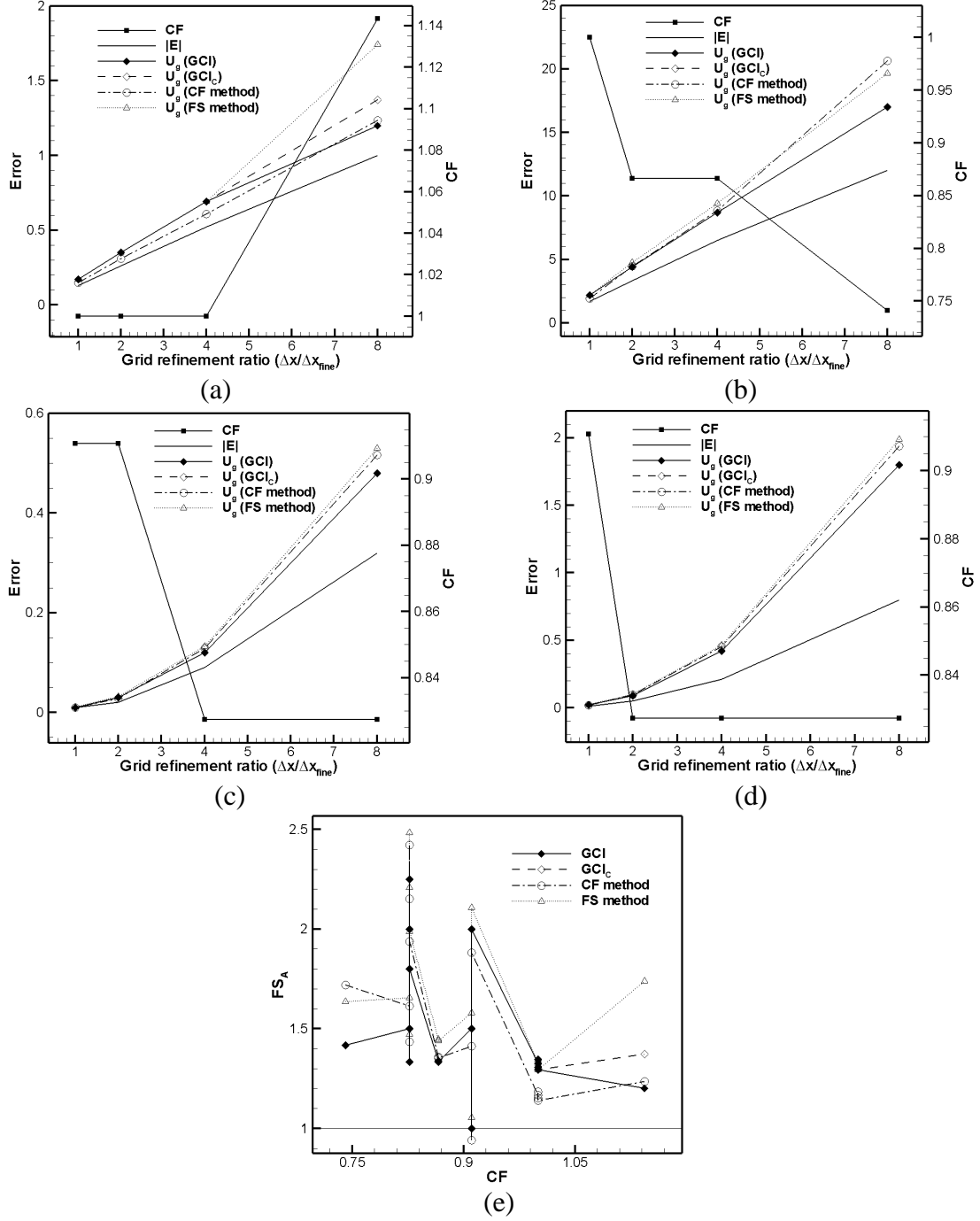
Figure A12: One-dimensional steady-state convection-diffusion process without source term, with constant transport properties and with Dirichlet boundary conditions, Pe=1 and Pe=10 [11]: (a) UDS-Pe=1, (b) UDS-Pe=10, (c) SMART-Pe=1, (d) SMART-Pe=10, (e) actual factor of safety.
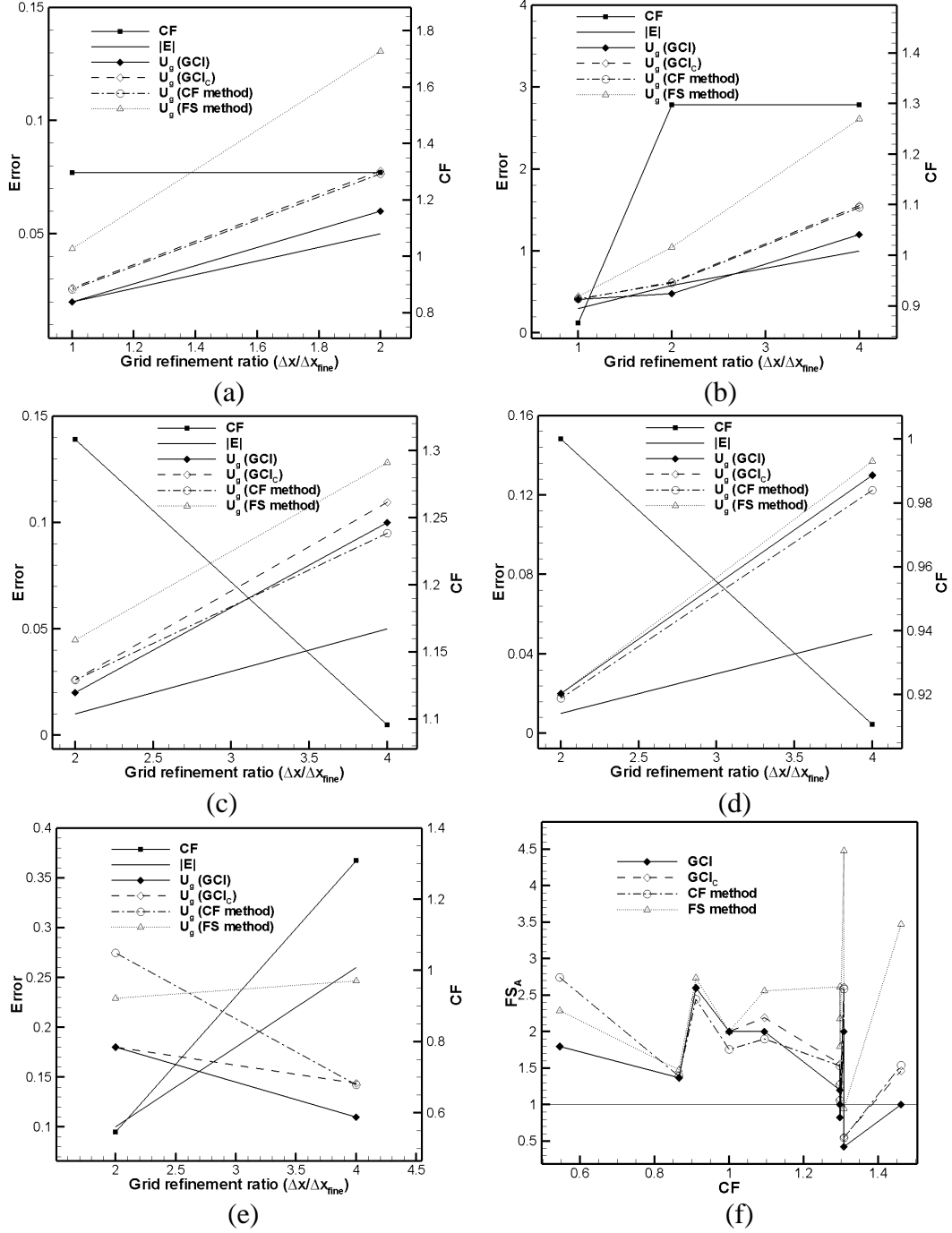
Figure A13: Heat transfer from an isothermal cylinder enclosed by a square duct [27, 28, 29]: (a) UDS-y-velocity, (b) UDS-temperature, (c) SMART-x-velocity, (d) SMART-y-velocity, (e) SMART-temperature, (f) actual factor of safety.

(a)

(b)

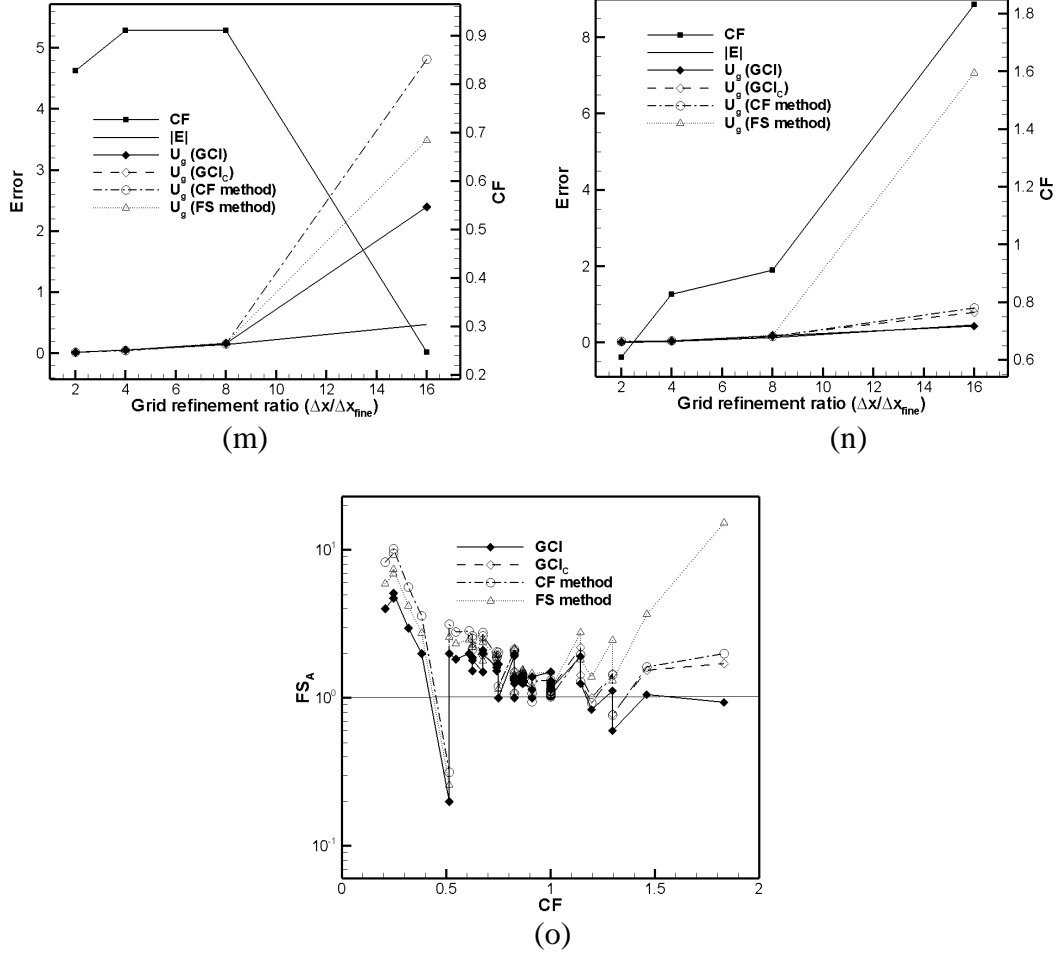(c)

(d)

(e)

(f)

(g)

(h)

(i)

(j)

(k)

(l)
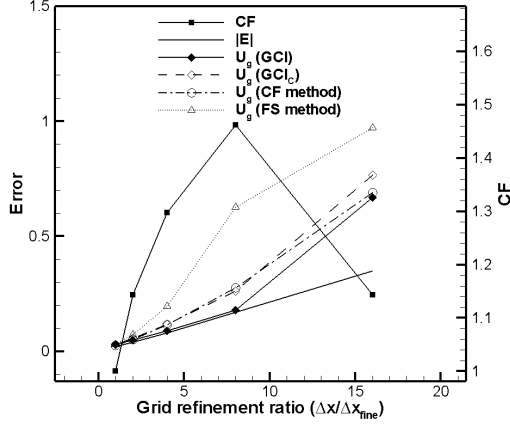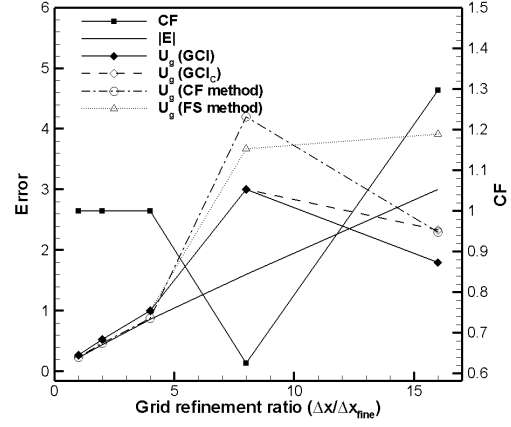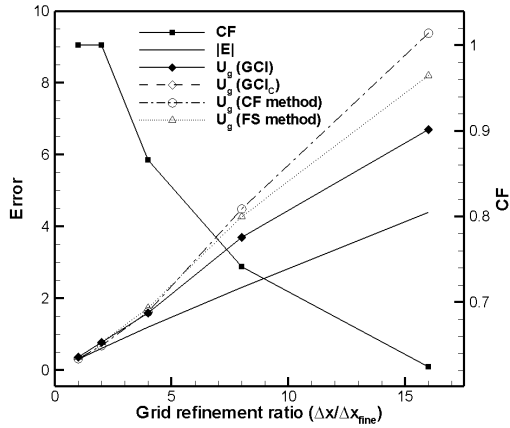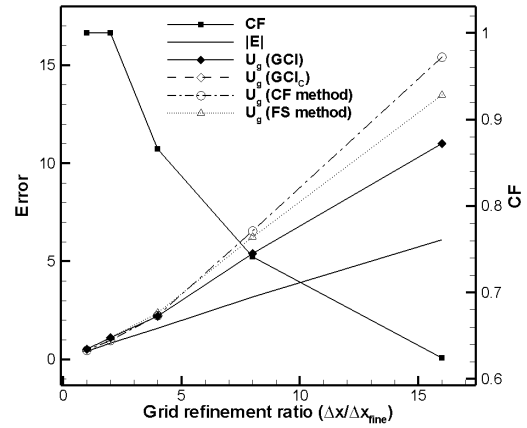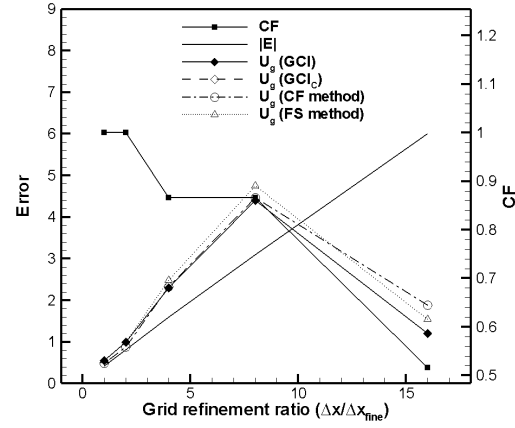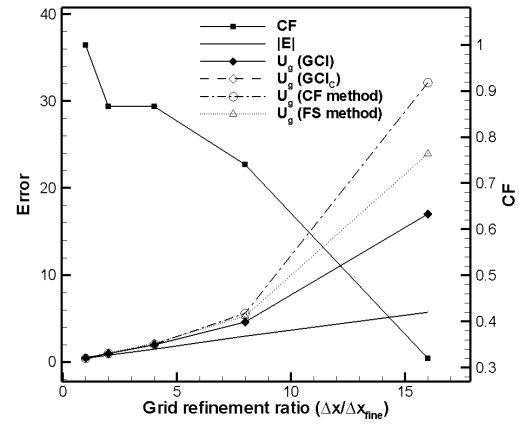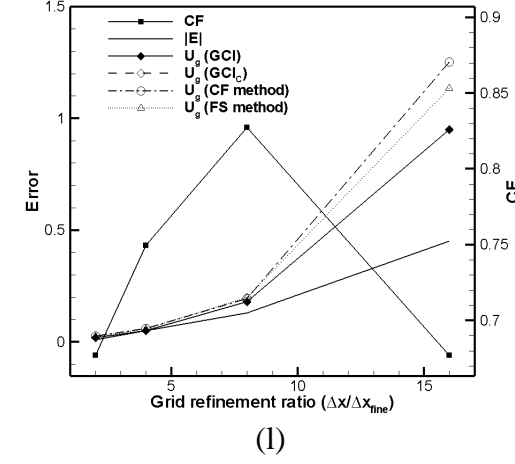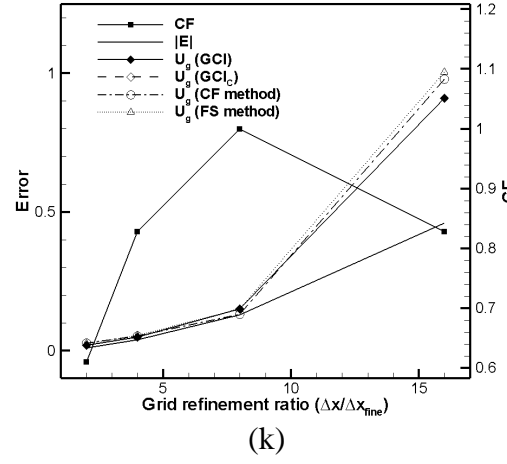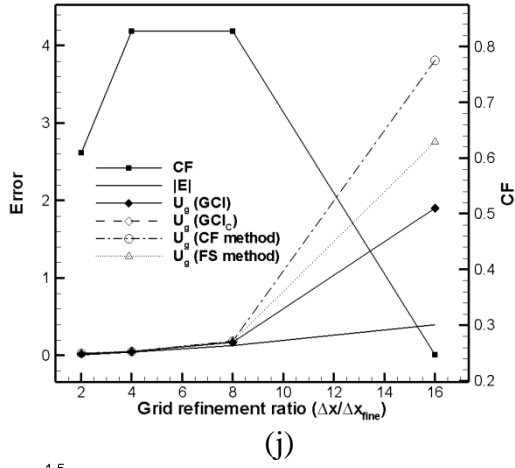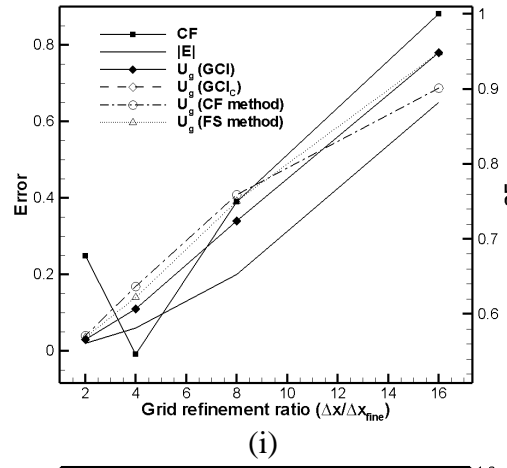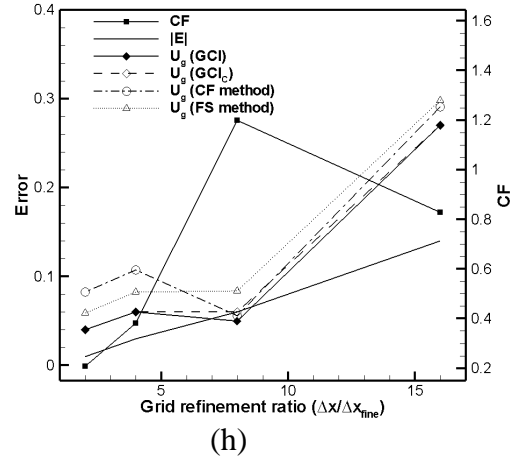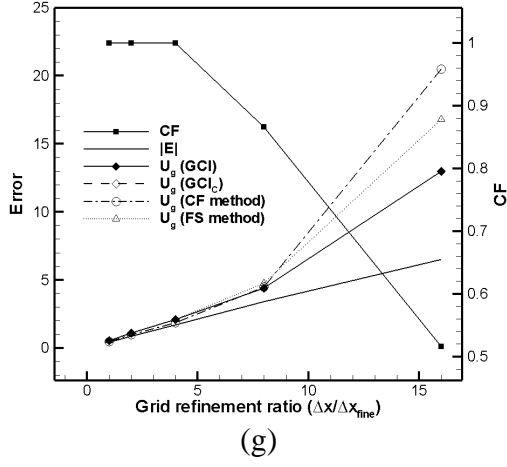
Figure A14: Premixed methane/air laminar flat flame on a perforated burner [28, 30, 31]:
(a) UDS-radial-velocity, (b) UDS-axial-velocity, (c) UDS-temperature,
(d) UDS-CH4, (e) UDS-O2, (f) UDS-CO2, (g) UDS-H2O, (h) SMART-
radial-velocity, (i) SMART-axial-velocity, (j) SMART-temperature,
(k) SMART-CH4, (l) SMART-O2, (m) SMART-CO2, (n) SMART-H2O,
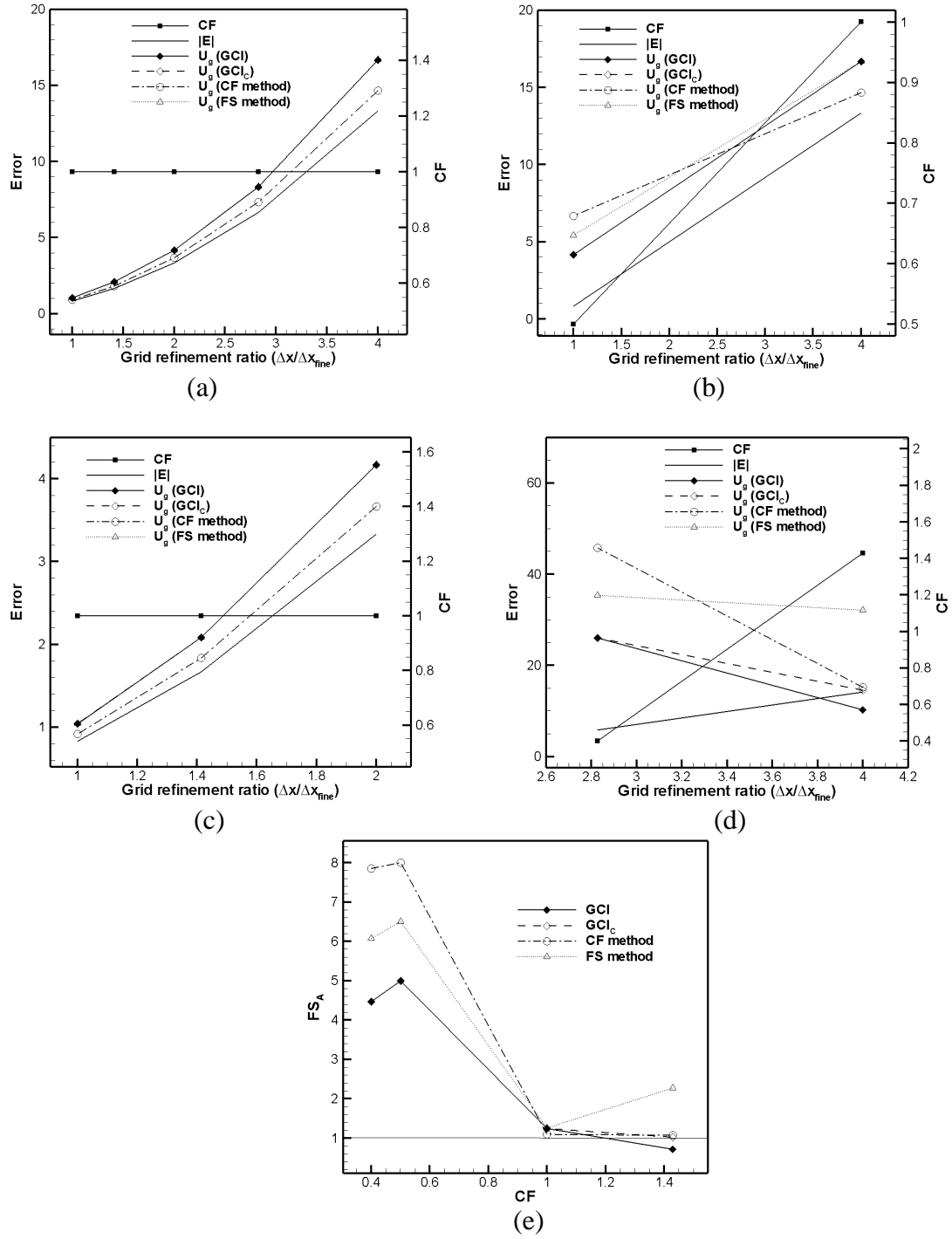(o) actual factor of safety.

Figure A15: Data for "exact" grid convergence set [8]: (a) exact to F=600, (b) perturbed #3, (c) perturbed #4, (d) all±5, (e) actual factor of safety.
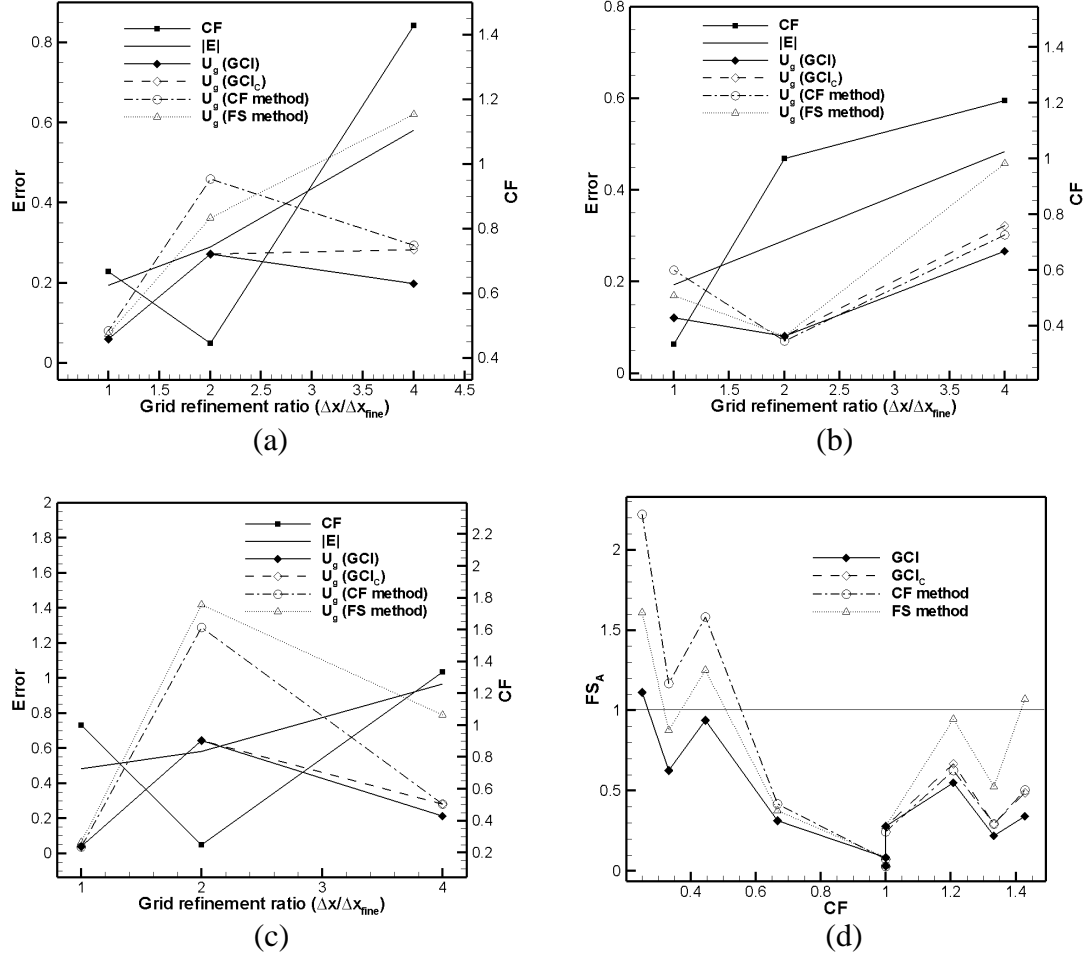
Figure A16: Beam bending problem for 2nd series on grid convergence [8]: (a) beam bending stress (Code 1), (b) beam bending stress (Code X), (c) beam bending stress (Code W), (d) actual factor of safety.
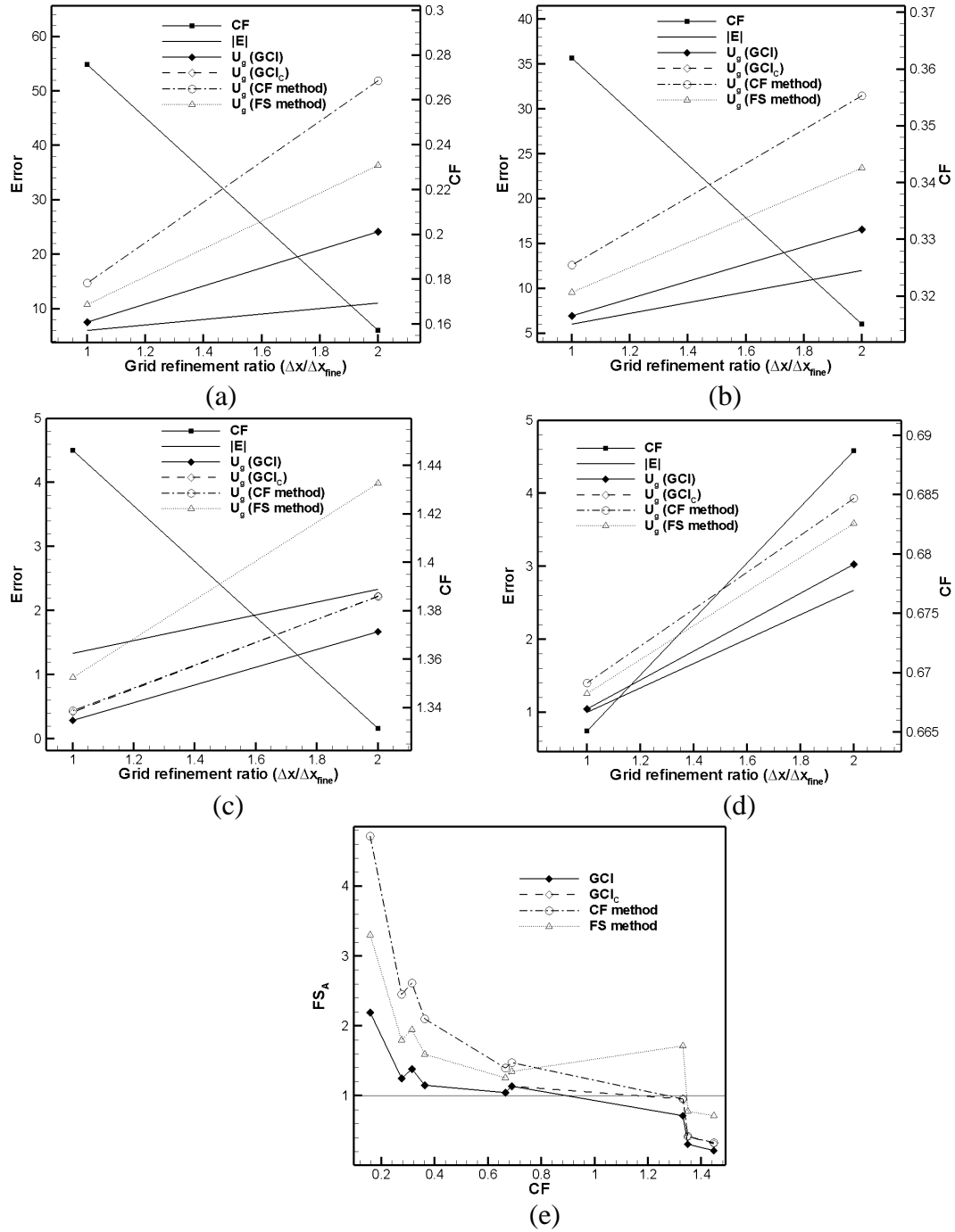
Figure A17: Beam bending problem for 3rd series on grid convergence [8]: (a) beam bending stress (Code 1, code X), (b) beam bending stress (Code W), (c) Beam end deflection (Code 1), (d) Beam end deflection (Code X), (e) actual factor of safety.